Anatomy of an Extreme Event

Martin Hoerling[1], Arun Kumar[2], Randall Dole[1], John W. Nielsen-Gammon[3], Jon Eischeid,[1,4], Judith Perlwitz[1,4], Xiao-Wei Quan[1,4], Tao Zhang[1,4], Philip Pegion[1,4], and Mingyue Chen[2]

[1]NOAA Earth System Research Laboratory, Boulder, Colorado

[2] NOAA Climate Prediction Center, Camp Springs, MD

[3] Department of Atmospheric Sciences, Texas A&M University, College Station, Texas

[4] University of Colorado, Cooperative Institute for Research in Environmental Sciences, Boulder, Colorado

Submitted to *J. Climate*

10 May 2012

Revised

18 October 2012

Corresponding author address: M. Hoerling, NOAA/Earth System Research Laboratory, 325 Broadway, Boulder CO 80305.
E-mail: martin.hoerling@noaa.gov

ABSTRACT

The record-setting 2011 Texas drought/heat wave is examined to identify physical processes, underlying causes, and predictability. October 2010-September 2011 was Texas's driest 12-month period on record. While the summer 2011 heat wave magnitude (2.9°C above the 1981-2010 mean) was larger than the previous record, events of similar or larger magnitude appear in pre-industrial control runs of climate models. The principal factor contributing to the heat wave magnitude was a severe rainfall deficit during antecedent and concurrent seasons related to anomalous sea surface temperatures (SSTs) that included a La Niña event. Virtually all the precipitation deficits appear to be due to natural variability. About 0.6°C warming relative to the 1981-2010 mean is estimated to be attributable to human-induced climate change, with warming observed mainly in the past decade. Quantitative attribution of the overall human-induced contribution since pre-industrial times is complicated by the lack of a detected century-scale temperature trend over Texas.

Multiple factors altered the probability of climate extremes over Texas in 2011. Observed SST conditions increased the frequency of severe rainfall deficit events from 9% to 34% relative to 1981-2010, while anthropogenic forcing did not appreciably alter their frequency. Human-induced climate change increased the probability of a new temperature record from 3% during the 1981-2010 reference period to 6% in 2011, while the 2011 SSTs increased the probability from 4% to

23%. Forecasts initialized in May 2011 demonstrate predictive skill in anticipating much of the SST- enhanced risk for an extreme summer drought/heat wave over Texas.

1. Introduction

Drought and heat are no strangers to Texas. According to climate division data from the National Climatic Data Center (NCDC; Guttman and Quayle, 1996), the average summertime (June through August) temperature is higher in Texas than in any other of the lower 48 states. Memorable Texas summertime heat waves include 1934 during the Dust Bowl, the 1980 central United States heat wave with 107 heat-related deaths reported in Texas (Greenberg et al., 1983), and the more localized Texas-Oklahoma heat wave in 1998 (Hong and Kalnay, 2002). The drought of 1948-1957 is the drought of record across most of Texas, and the statewide Palmer Drought Severity Index (PDSI) achieved a minimum of -7.80 in September 1956. Other memorable droughts and their associated minimum PDSI values were in 1916-1918 (-7.09) and 1925 (-6.10).

And then came 2011. The three-month average for June through August was 30.4 °C, warmer than any previous single month. This was 2.9 °C above the long-term average, nearly a factor of two larger than the previous record June-August departure. The heat was accompanied by extreme drought: statewide precipitation for October 2010 through September 2011 was 287 mm, a new record for driest consecutive twelve months. The PDSI reached a new record minimum of -7.93 in September 2011. Along with the drought and heat came record statewide agricultural losses of $7.62 billion (Fannin, 2012). Wildfires burned 3,993,716 acres, almost double the previous highest value in twenty years of statewide records, according to the Texas Forest Service. Commercial timber losses from the

drought totaled $755 million, of which only 13% was due to wildfire (Texas Forest Service, 2012).

This paper examines the climatological context for both the extreme precipitation and temperature conditions occurring over Texas during 2011, it diagnoses the physical processes contributing to both conditions including their interrelationship and feedbacks, and it examines underlying causes with a principal purpose to provide a predictive understanding (i.e., quantify the predictability). The paper assesses how various contributing factors affected event occurrence, including its timing and location, but especially its magnitude and probability for record threshold exceedence, comparing the role of natural factors to those associated with human-induced climate change. In addition to the analysis of observational data, the paper diagnoses initialized coupled forecasts that were part of NOAA's operational seasonal forecasting activities, and uninitialized climate simulations of the Coupled Model Intercomparison Project Phase 5 (CMIP5).

Several specific questions are considered in this study of the 2011 Texas drought and heat wave. What processes, whether due to natural variability or anthropogenic climate change, might have provided early warning? Were, for instance, interannually-varying sea surface temperatures (SSTs) important, as for the 1998 heat wave (e.g. Hong and Kalnay 2000), and to which the 1930s and 1950s Central U.S. warm/dry epochs were also sensitive (Schubert et al. 2004a,b; Seager et al. 2005; Hoerling et al. 2009)? Did soil moisture play an appreciable role in this

event, given that the Great Plains is a region of known strong land surface feedbacks on summertime air temperature and rainfall (e.g. Koster et al. 2004, Krakauer et al. 2010) and case studies provide evidence for appreciable soil moisture effects in 1980, 1998 and during the Dust Bowl (e.g. Hong and Kalnay 2002, Lyon and Dole 1995; Schubert et al. 2004a,b)? How did the antecedent deficits in precipitation, which themselves were record setting, influence the subsequent summer Texas heat wave intensity in light of global observational analyses indicating that hot summer days are much more likely after the occurrence of precipitation deficits (Mueller and Seneviratne 2012)? And, what aspects of the drought/heat wave were manifestations of human-induced climate change?

Presented herein is a considerably broader assessment of the causes for the extreme Texas conditions than would be entailed by an attribution of human-induced climate change alone. Likewise, the study is concerned not just with how various factors, including anthropogenic climate change, may have altered the probability of exceeding a particular extreme threshold for rainfall and temperature over Texas in 2011, but also with explaining the full magnitude of the drought and heat wave intensities.

Statistical analyses of the relationships between climate change and general classes of events may provide some gross insights on the Texas drought/heat wave event, but there are significant uncertainties. For instance, warm extremes have increased more rapidly in recent decades compared to cold extremes over the

United States as a whole (Meehl et al. 2009), and a recent synthesis report expresses medium confidence that heat waves have lengthened and become more frequent over many regions as a result of anthropogenic climate change (IPCC, 2012). Yet, no systematic changes in the annual and warm season mean daily temperature have been detected over the Great Plains and Texas over the 62-year period from 1948-2009 (Groisman et al. 2012) consistent with the notion of a regional "warming hole" (e.g. Kunkel et al. 2006). Indeed, May–October maximum temperatures over the region have decreased by 0.9°C (62 yr)-1 which is statistically significant according to Groisman et al. The authors surmise that "It may well be that the maximum temperature decrease was caused by wetter warm seasons in the last decades rather than an opposite inference". Their assessment of an increase in regional summertime rainfall is consistent with results of a century-scale analysis that also shows significant increases in precipitation (McRoberts and Nielsen-Gammon 2011), and with the IPCC (2012) report on extremes that notes droughts have become less frequent, less intense, and shorter in duration since about 1950 over central North America.

It is therefore evident that neither the 2011 record drought nor record heat wave were consistent with recent regional trends over Texas, complicating the quantification of overall human-induced climate change contribution. Thus, a comprehensive event-specific diagnosis, including assessing its climatological context in both a regional and global framework, is essential for a proper understanding of this extreme event.

The paper presents a quantitative analysis into the anatomy of the 2011 Texas heat wave and drought, undertaken in the spirit of Namias's (1982) dissection of the 1980 event. Section 2 describes the observational and numerical model data sets. Section 3 probes into potential causes for the climate extremes including an assessment of the range of extremes that could arise solely from natural variations and a quantification of the likely roles of both natural and human influences on the drought and heat wave. The paper contrasts the ability of uninitialized and initialized climate models in simulating the extreme conditions over Texas during summer 2011. A summary of results is presented in section 4 which includes a discussion of the possible overall effects of climate change over the period spanning pre-industrial times to the present.

2. Data and Methods

a. Observational data

Contiguous U.S. surface temperature and precipitation for 1895-2011 are derived from NOAA's monthly U.S. Climate Division data (NCDC 2002). Analyses of Texas averaged conditions are constructed by averaging the 10 individual climate divisions available for the state. Global monthly SST data is based on the 1° gridded HadISST product (Rayner et al. 2003). For both datasets, seasonal departures are calculated relative to a 1981-2010 reference.

b. Climate model simulations

Four configurations of climate simulations are studied in order to determine different aspects of the variability in Texas temperature and rainfall. One employs a suite of CMIP5 global coupled ocean-atmosphere models in which external radiative conditions are fixed to pre-industrial conditions. We analyze the results from 18 different models having integrations typically on the order of 500 years. A more detailed analysis is conducted of a dataset consisting of 1500 years of simulations based on the fourth version of the Community Climate System Model (CCSM4; Gent et al. 2011). This and other model configurations are summarized in Table 1.

A second configuration employs a global atmospheric model in which SSTs, sea ice, and carbon dioxide concentrations (but no other external forcings) are specified to vary as observed during the period 1950-2010. This uses the atmospheric component (GFS) of the second version of NOAA's Climate Forecast System (CFSv2). Further, in order to assess the statistical properties of the atmospheric response to global SST/sea ice conditions during the period of the Texas heat wave, we examine output from a third additional 80-member ensemble of GFS simulations spanning the period October 2009 thru September 2011.

The fourth configuration is based on the externally forced CMIP5 simulations. We analyze monthly output from 20 different models which were subjected to variations in greenhouse gases, aerosols, solar irradiance, and the radiative effects of volcanic activity for 1880-2005 (Taylor et al. 2012). Our analysis uses single runs from each of the modeling centers.

225

226 *c. Climate model projections and predictions*

227 *Projections* (uninitialized simulations) of climate conditions during the 2011 Texas
228 heat wave are based on CMIP5 models employing the Representative Concentration
229 Pathway 4.5 for individual greenhouse gases and aerosols (Moss et al. 2010). We
230 diagnose the CMIP model runs for an 11-year centered window (2006-2016) in
231 order to consider a large ensemble from which the model's signal and the intensity
232 of natural internal variability in 2011 can be estimated. The forcing will be
233 subsequently referred to as "anthropogenic forcing" to denote the radiative driving
234 associated with the projected changes in anthropogenic GHGs and aerosols, and the
235 impacts for 2011 will be referred to as "human-induced" climate change.

236

237 *Predictions* (initialized forecasts) of climate conditions are analyzed using the first
238 (CFSv1; Saha et al. 2006) and second (CFSv2) generations of NOAAs climate forecast
239 system. Apart from differences in the resolution of the atmospheric and oceanic
240 component models between CFSv1 and CFSv2[1], another difference is that the CO_2
241 conditions for the CFSv1 were held fixed at their 1988 values for all hindcasts and
242 real-time forecasts, while CFSv2 has a time-evolving CO_2 concentration. For each
243 system, retrospective forecasts (hindcasts) provide a reference from which forecast
244 anomalies for 2011 are calculated. All predictions are for JJA seasonal means based
245 on initialization from May conditions. Table 1 provides details on the hindcast and
246 forecast procedures.

[1] *The atmospheric component of CFS, the Global Forecast System (GFS) uses a spectral truncation of 62 and 126 waves in version 1 and 2 respectively.*

The monthly temperature and precipitation data from all model simulations, projections and predictions are interpolated to the 344 NCDC U.S. Climate Division centroids using a simple linear inverse distance technique to facilitate comparison with the observations. Texas averages are calculated as the area-weight of the 10 climate divisions defining the state. Unless stated otherwise, all model and observed anomalies for 2011 conditions are calculated relative to a 1981-2010 reference climatology. There are several reasons for using this 30-year period. First, the various model and observed data sets have as their common period of evaluation 1981-2010, thus making this the only period for meaningful intercomparison. Second, it is standard practice in climate monitoring to use a 30 year period as it is long enough to filter out interannual variations, but also short enough to be able to respond to longer climatic trends. Finally, operational practices of seasonal forecasting involve articulating anomalies relative to the most recent 30-year average. An assessment of observed overall climate trends spanning the longer period of historical data is also presented, and section 4 further discusses estimates of the overall anthropogenic climate change signal in which the period of reference for estimating CMIP5 model simulations for 2011 is the models' pre-industrial climate.

3. Results

The 2011 heat wave was centered over Texas and Oklahoma (Fig. 1, top), and included western portions of Louisiana and Arkansas, southern Kansas, and eastern New Mexico. The Texas summer temperature of 30.4°C in 2011 was an outlier with respect to conditions during 1895-1954 that included the Dust Bowl era and the sustained late 1940s/early 1950s drought period. It was also an outlier relative to the recent epoch of 1955-2010 that includes the era of rapidly increasing atmospheric greenhouse gas concentrations as indicated in the probability distribution functions (PDFs) of summertime temperature (Fig. 1, bottom right). The similarity in statistical properties of Texas summer temperatures between 1895-1954 and 1955-2010 is consistent with the lack of an appreciable summertime warming trend over the Southern Plains since the beginning of the 20th Century (e.g. Kunkel et al. 2006; Fig 1, bottom left). The extreme magnitude of the 2011 event thus would not have been anticipated from any appreciable century-scale trend in the historical time series of Texas summer mean temperatures or their variability, similar to the situation that occurred in relation to the 2010 Russian summer heat wave (Dole et al. 2011). Likewise, the severe deficits in precipitation during 2011 would not have been anticipated from century-scale trends, which were actually toward wetter conditions (McRoberts and Nielsen-Gammon 2011).

a. The role of randomness

We address the question whether an event as extreme as occurred in 2011 might have been anticipated (at least in a statistical sense) if a longer-term record were available. In such a case, relying on a limited observational data record could result in significantly underestimating the probability of an extreme heat wave or, put another way, overestimating how rare such events would be. This is precisely the recipe for a "climate surprise".

We test this possibility by calculating the statistics of 100-year block maxima for Texas summertime temperatures occurring in the pre-industrial simulations of CMIP5. Figure 2 shows the histogram (gray bars) of the 115 hottest summers occurring in consecutive, non-overlapping 100-year samples. There is substantial variability in the magnitude of 1 in 100 year summer warm extremes in these simulations, ranging from a low value of +1.2°C departure to a high value of +4°C departure. The observed 2011 event is thus seen to fall well within this distribution, which also brackets the values for the observed 1895-2010 prior record. The fact that 2011 had a heat wave magnitude much greater than occurring in the prior 116-yr observational record could thus be reconciled, at least in part, with the inadequacy of observational data and sampling noise. There are uncertainties, however, in the CMIP5 estimates of such extreme Texas heat wave magnitudes stemming in part from the fact that individual models have interannual variability of Texas summer temperatures that is appreciably greater than and also some that is appreciably less than observed. The histogram should therefore not be

viewed as having been drawn from a homogeneous population. Several individual models having long integrations (on order of 1000 yrs) also yield spreads in their 100-yr block maxima heat waves analogous to that shown for the entire multi-model distribution. In particular, a 1500-yr long simulation of CCSM4 was analyzed separately, in part because of the excellent model representation of climatological mean summer Texas temperatures (27.8°C compared to 27.4°C observed) and the realism of its interannual variability (standard deviation of 0.8°C compared to 0.7°C observed). The range among the 15 samples of CCSM4 block maxima heat waves was +1.5°C to +3°C, consistent with the multi-model spread.

The range of 100-yr block maxima extreme event magnitudes is almost certainly greater than indicated by the histogram alone, the latter having been drawn from a finite sample of the models' population. Figure 2 addresses this further by superposing upon the histogram two probability distribution functions, one is a fitted Gaussian (red curve), and the other is a non-parametric fit. It is evident that the Gaussian curve is not a particularly good fit to these extreme values, consistent with expectations from Generalized Extreme Value theory, though again the fact that the data are not drawn from a homogeneous population sample must be recognized also. Whether based on the histogram or the curve fits, the results in Fig. 2 suggest that natural variability alone appears capable of producing heat wave magnitudes as large (or larger) than observed in 2011.

To have illustrated, based on CMIP5 simulations, that natural variability appears capable of producing extreme heat waves as large as or larger than observed in

2011 is of course not the same as stating that natural variability accounts for the total observed magnitude of this particular event. This does, however, confirm that the observed 116-year record is insufficient to delineate the extremes of natural variability.

The extreme heat waves in the CMIP5 simulations, though statistically random events, were accompanied by a coherent pattern of global SST evolution. To illustrate the evolution of such a pattern , we use the very large sample of CCSM4 runs. In addition to the attributes of having a realistic Texas region climatology, this model is also suitable for analysis because of the realistic pattern of tropical SST variability (Gent et al. 2011), to which Texas climate is well-known to be sensitive. Figure 3 (top panels) shows the composite global SST and U.S. precipitation anomalies that were coincident with the summertime occurrences of the 1 in 100 year heat wave events. Extreme Southern Plains dryness is seen to accompany these heat waves, as was noted also in 2011 and during past Texas heat waves. Dryness is also noted in the model over the Pacific Northwest, though these departures, shown as standardized anomalies, are small in an absolute sense because they occur during that region's climatological dry season. The JJA SST anomalies in the tropical equatorial Pacific are not particularly extreme, though they are part of a pattern typical of the waning phases of La Niña events, including cool tropical/subtropical SSTs in most basins, and a distinctive North Pacific SST anomaly pattern. Antecedent October-May SST composite conditions for these heat wave events illustrates a mature La Niña structure (Fig. 3, bottom left), and a similar La Niña

pattern occurs in several other CMIP5 models that were examined (not shown). Likewise, the antecedent U.S. precipitation anomaly pattern (Fig. 3, bottom right) shows dryness over Texas and the Gulf Coast region, a feature that is consistent with known global climate anomalies associated with La Niña (e.g. Kiladis and Diaz 1989). A similar evolution of cold Pacific SSTs accompanied the 2011 Texas heat wave, and the combination of antecedent and contemporaneous dryness were likewise particular features of the 2011 Texas heat wave. It should be noted that the tropical Atlantic SSTs in the CCSM4 heat wave composite for pre-industrial runs are cold, which is opposite to the warm conditions occurring during the 2011 heat wave, as discussed further in the next section.

b. The role of forcing

Suites of climate simulations are diagnosed to address how anthropogenic forcing, SST forcing, and soil moisture forcings contributed to the 2011 extreme event. It should be noted that SST and soil moisture conditions in 2011 likely possess some anthropogenic component, aspects of which are discussed further below. Figure 4 illustrates the observed pattern of global SST anomalies for summer 2011 (top, left), and for the preceding seasons (bottom, left). The pattern of SST anomalies are similar to known patterns of natural coupled ocean-atmosphere variability. For instance, the antecedent conditions consisted of tropical Pacific cold SSTs with peak anomalies of -1.5°C, a horseshoe pattern of warm anomalies stretching poleward from the equatorial west Pacific, and cold anomalies extending along the west coasts of North and South America that are characteristic of a mature La Niña event. The

tropical SST anomalies weakened considerably by summer as La Niña waned. On the other hand, warm SST anomalies exceeding +0.5°C that covered the tropical Atlantic Ocean throughout this period were atypical of La Niña. The 2011 warmth of the tropical Atlantic Ocean was more likely related to a combination of lower frequency behavior that may have included natural multi-decadal Atlantic variability and an externally forced global warming trend (Ting et al. 2009).

While no explicit experiments are conducted in this study that constrain evolution of soil moisture, cumulative precipitation serves as a proxy indicator for soil moisture. The U.S. summer 2011 precipitation departures (Fig. 4, right top) and the antecedent deficits accumulated during the prior eight months of the water year (Fig. 4, right bottom) were less than 50% of normal, each breaking records for their driest periods since 1895. These dry conditions are contrary to observed long-term trends in the region which consist of decreased dryness, droughts becoming less frequent, less intense, and shorter in duration (IPCC 2012).

It is not surprising that the hottest summer coincided with the driest summer over Texas in 2011 given the well-known inverse correlation between temperature and precipitation over this region (e.g. Madden and Williams 1978) and various other evidence for strong soil moisture feedbacks on summer climate (e.g. Senevirante et al. 2006; Fischer and Schar 2010; Hirschi et al. 2011). Yet, the extreme magnitude of the heat wave cannot be reconciled with the extreme summer dryness alone, at least not in a linear sense. Despite the strong inverse relation between Texas summer

rainfall and temperature (Fig. 5), a prediction based on this historical data fails to anticipate the extreme magnitude of the summer temperature when accounting for the extreme coincident precipitation deficit. This is indicated by the large displacement between the JJA 2011 observed conditions and the linear fit, even giving reasonable consideration for the scatter about the linear relation.

There is reason to posit that the relation between temperature and precipitation may be a nonlinear function of the soil moisture deficit, for instance as found during summer over southeastern Europe (Hirschi et al. 2011). Also, analyses of historical Texas temperature and precipitation data by Mueller and Senevirante (2012) find an asymmetrical impact of antecedent drying on the probability of hot summer days, with the hot tail of the temperature distribution more affected by precipitation/soil moisture deficits. Furthermore, aside from the predictive component of temperatures related to antecedent soil moisture impacts, there is also a potential impact of human-induced warming over Texas in 2011.

Figure 6 compares the June-August 2011 observed contiguous U.S. precipitation and surface temperature anomaly patterns (top) with the ensemble mean anomalies from the AMIP (middle) and CMIP5 (bottom) simulations (relative to 1981-2010). The forced response to the actual SST conditions capture several of the principal regional features of the 2011 climate conditions. The AMIP simulations indicate, in particular, that the pattern of above normal temperature and below normal rainfall focused on the Texas area was part of a regional sensitivity to that year's SST

conditions. Cold tropical Pacific SSTs were likely an important factor in causing southern Plains dryness as affirmed in model experiments that have assessed U.S. climate sensitivity to separate ocean basin forcing (e.g. Schubert et al. 2009). Likewise, climate experiments studied by Findell and Delworth (2010) reveal that warm tropical Atlantic SSTs also contribute to southern Plains drying, though that sensitivity is weaker than the influence of tropical Pacific SSTs.

In contrast, no such regional specificity emerges in response to the anthropogenic forcing alone. The CMIP5 simulations indicate a mostly uniform surface warming response that spans the entire contiguous U.S., indicating that the Texas region was not particularly susceptible (relative to adjacent regions) to the change in anthropogenic forcing. Further, there is no material sensitivity of summer mean precipitation to the anthropogenic forcing over the U.S. as a whole for 2011. Nor do the CMIP5 simulations indicate appreciable sensitivity of antecedent winter and spring precipitation over the U.S. (not shown).

The AMIP forced experiments suggest that a +1.1°C warm signal existed during summer over Texas as a consequence of the particular global ocean conditions in 2011, which implies approximately 40% of the magnitude of the Texas heat wave (+2.9°C) might have been anticipated as a mean response to forcing related to the specific ocean conditions. The CMIP forced experiments further suggest that a +0.6°C warm signal existed during summer over Texas as a consequence of the projected anthropogenic GHG and aerosol conditions in 2011, which implies that

relative to 1981-2010 about 20% of the magnitude of the Texas heat wave might have been attributable to such forcings. The characteristcs of these PDFs are summarized in Tables 2 and 3, and discussed further in section 3d. Suffice it to state here that the forcing associated with observed SSTs greatly increased the probability for an extreme dry and hot summer over Texas in 2011, considerably more so than did anthropogenic forcing.

To what extent can the seasonal responses in the AMIP and CMIP simulation suites be interepreted as representing separate and independent forcing effects? While much of the pattern of ocean conditions in 2011 was consistent with natural internal variability, some fraction of the anomaly patterns likely also included a climate change component, and as such the AMIP responses are not necessarily signatures of internal ocean variability alone. Regarding rainfall, however, the results do lend themselves to an interpretaton of seperate physical forcing factors. In particular, the AMIP simulated drying over the Texas region is likely due to natural SST forcing alone insofar as the CMIP simulations do not yield a discernible precipitation response. This is consistent with the results of other modeling studies that find the global SST trends produce only weak precipitation responses over the continental U.S. (Schubert et al. 2009). Regarding temperature, the AMIP simulated warming over the Texas region likely includes a human-induced component via anthropogenic forcing of SSTs, however, the majority of the AMIP simulated warmth resulted from the aforementioned drying signal and the physical relationship between precipitaiton deficits and hot summers (e.g. Mueller and Senevirante 2012)

The Texas warming in the CMIP simulations is partly due to the direct effect of changed radiative forcing on the region's temperature (a factor not included in the AMIP simulation for 2011), and an indirect effect related to human-induced ocean warming (Hoerling et al. 2006, 2008; Dommenget 2009; Compo and Sardeshmukh 2009).

How robust are the signals derived from this particular suite of model simulations? The structural uncertainty in each signal that would arise from model biases cannot be determined from the present suite of model runs. In particular, additional experiments employing different atmospheric models also run in AMIP mode would need to be analyzed to assess the uncertainty in SST/sea ice signals. Likewise, ensembles of each of the 20 CMIP5 models would be required to estimate the uncertainty in the human-induced climate change response. The current study provides a single indication of the probable human-induced signal in 2011 climate conditions, derived by ensemble averaging single runs of each CMIP model. Additional analyses described further below, however, suggest that this CMIP5 ensemble mean signal is a reasonable estimate of the anthropogenic forcing of Texas summertime temperatures, at least for 2011 relative to 1981-2010.

Aside from estimating the mean value of the forced response, it is also important to diagnose the variability about that mean and thereby assess how deterministic the 2011 Texas extreme event was with respect to forcing. Was the observed occurrence of an extreme heat wave and drought the only outcome possible over Texas in 2011 for the particular conditions of boundary and external forcings? Was

it the most likely outcome? Could the JJA 2011 conditions have been even more severe? To address such questions , Fig. 7 shows the frequency distributions of the simulations of JJA 2011 and of the reference period 1981-2010 for AMIP (top) and CMIP5 (bottom). The considerable spread evident in each of the probability distribution functions (PDFs) reveals the appreciable role of random variability in Texas summer climate. For instance, consider the PDFs for 2011 based on the AMIP simulations. Because each of the 80 members was identically forced, the spread of the distributions is entirely due to internal atmospheric noise. Thus, while the odds of a cold summer were much reduced in 2011 compared to 1981-2010, three of the model simulations did produce colder than normal summer conditions over Texas in 2011. The CMIP5 spread for 2011 simulations is greater than the AMIP spread in part because the latter is constrained by a single particular SST conditions, but also because the former has overall greater summertime temperature variability (see Table 3), and an even larger fraction of CMIP5 runs yielded cold summer conditions over Texas in 2011. The important indication offered by these PDFs is that a wide range of possible climate outcomes for Texas in 2011 would have been consistent with, and thus possible under, the influences of forcings. In particular, the observed extreme hot temperature and drought conditions were not the most probable outcomes in 2011, even though the probability of such extremes was greatly increased owing especially to the SST conditions of 2011 (see section 3d). These results once again suggest the important role played by random internal variability, consistent with our analysis of the pre-industrial climate simulations.

c. Physical process understanding

Here we examine the relationship between Texas summertime temperature and precipitation variability in the context of how their linkages may have been sensitive to the influence of the specific 2011 SST and GHG forcings. Diagnosis of AMIP and CMIP models is conducted to specifically test whether precipitation deficits amplified the hot tails of the summertime temperature distribution. An intercomparison of these forced experiments will also address how the observed record-breaking heat wave arose from physical processes tied to naturally varying ocean conditions versus those tied to increased greenhouse gase and aerosol concentrations. Regarding effects of the latter forcings, the question of detection of a human-induced climate change over Texas is also explored, despite the absence of a century-long warming (or drying) over Texas noted in the prior section.

Figure 8 presents the scatter relationship between Texas summer temperature and rainfall in AMIP (top) and CMIP (bottom) simulations for both the 1981-2010 reference period (left) and the actual forcing conditions of 2011 (right). A strong negative correlation between temperature and rainfall, with a magnitude quite similar to that found in observations, occurs in all the simulation suites. Having the advantage of a large sample of model realizations (720 for CMIP; 360 for AMIP), one can discern nonlinearity in the temperature/rainfall relationship occurring at the tails of the distribution. This is characterized by a larger sensitivity of Texas summertime temperature per incremental precipitation change for dry conditions compared to wet conditions. We also note that the CMIP5 samples include several

heat wave occurrences larger in magnitude than the 2011 event during 1981-2010, consistent with the appreciably greater variance in surface temperature in CMIP5 models than is observed (see Table 2).

It is plausible therefore that amplification of the hot tails of the summertime temperature distribution was an important physical process associated with the extreme 2011 Texas event. Additional evidence to this effect is seen in the scatter relationships for the model simulations of summer 2011. Note in particular that virtually all AMIP realizations were warm *and* dry (Fig. 8, top right). A small cluster of AMIP realizations produced summertime temperature departures near the observed heat wave magnitude, and these realizations were also among the driest. By contrast, the 2011 CMIP5 scatter is characterized by a shift in only the temperature probability relative to its 1981-2010 population. However, one again sees a few individual members as hot as observed, and these are also among the driest CMIP realizations. Severe drought thus appears to be a necessary ingredient for occurrences of Texas summertime extreme heat. While the SST forcing of 2011 increased the probability for below normal precipitation, it is important to recognize also the substantial random component of the summertime conditions over Texas as revealed by the PDF spreads in Fig. 7 and the scatter plot in Fig. 8. This is quantified in Table 2 which indicates that the AMIP mean drying signal of -34% was equivalent to only one standardized departure of the model's overall interannual variability.

We also find that SST forcing exerted an even greater effect on antecedent moisture conditions. Texas cumulative precipitation departures from October 2010 thru August 2011 (Fig. 9) are plotted for the 80-member averaged AMIP data (thick black line) and for observations (thick red line). About 80% of the magnitude of observed deficits accumulated during fall and winter can be explained by an SST-forced signal. Such antecedent dry conditions likely contributed significantly to the ensuing summer heat wave intensity, and perhaps also to the summer rainfall deficits themselves, as illustrated from further analysis of the very large ensemble of historical AMIP data. Shown in Fig. 10 is the model's Texas summer rainfall and precipitation sensitivity to October-May antecedent precipitation based on data from the 1950-2010 AMIP simulations, and a scatter plot is constructed from the 10% (72 sample) driest antecedents (red dots) and the 10% (72 sample) wettest antecedents. These simulations suggest several indications for land surface feedbacks, which may have contributed to the observed extreme summer conditions, though other factors (e.g. the SST evolution) could also have contributed. First, there is nearly a +2°C difference in the mean summer temperature between the dry versus the wet antecedent ensemble means. Also, the majority of dry (wet) antecedent cases experienced dry (wet) summers. And finally, there is a greater sensitivity of summer temperature to incremental rainfall departures in the environment of prior cumulative low moisture conditions compared to prior cumulative wet conditions, consistent with the nonlinearity seen in the temperature/precipitation scatter plots of Fig. 8. Recalling that the observed October-May 2011 Texas precipitation deficits were the most severe in the

historical record, these results imply that the probability for a record-breaking summer heat wave in 2011 (and also a further reduction in rainfall during summer) was strongly elevated by the antecedent drought as implied also by the empirical analysis of Mueller and Senevirante (2012).

We present two additional analyses that illustrate the significance of antecedent drought conditions of October – August 2011 on the subsequent summer temperature extremes. One is of the precipitation behavior in the subset of 2011 AMIP simulations that, by chance, produced the hot summer extremes in Texas having magnitudes close to the observed heat wave intensity. The precipitation evolution in these 8 runs (the 10% hottest) is indicated by orange lines in Fig. 9. It is apparent that all but one of the hottest realizations also experienced the most severe cumulative drought conditions for *both* antecedent *and* coincident periods, and that among all 80-members their particular rainfall traces were most similar to observations. A second analysis evaluates the Texas summertime temperature signal associated with such a particular condition --- both antecedent and coincident summer dryness--- but extracted from the much larger suite of historical AMIP runs. Shown in Fig. 11, this estimated "drought-induced temperature signal" is about +2°C, and the shift of the distribution relative to summertime temperatures unconditioned by precipitation is visibly apparent.

Finally, we consider the evidence for a human contribution to the 2011 Texas summer heat wave magnitude. The probability of hot summers has increased over

many land areas as a result of a human contribution to mean warming over the last century (e.g. Jones et al. 2008). But the southern Plains, sometimes referred to as a "warming hole" region, has been a noteworthy exception where no long-term warming has been observed (e.g., Kunkel et al. 2006; Knutson et al. 2006; Groisman et al. 2012), with such processes as natural variability (e.g., Wang et al. 2009), anthropogenic aerosols (e.g. Leibensperger et al. 2012), and land use change (e.g. Lawrence et al. 2011) being among various possible factors. One might thus argue that it is premature to attribute any fraction (large or small) of the heat wave intensity to effects of anthropogenic forcing in 2011, when in fact no long-term warming has been detected. Of course, to the extent that the lack of warming may be due to masking by strong natural variability rather than due to a lack of any climate change signal (e.g. Kunkel et al. 2006), then estimates of such signals via independent data (e.g, CMIP5 simulations) is valid. Some studies argue, however, that because of model biases, simulated regional climate responses to anthropogenic forcing may be unreliable over the Great Plains in summer (e.g., Pan et al. 2004). Also, long term regional climate trends are sensitive to the patterns of SST change (e.g., Hoerling et al. 2010; 2012), and as such, biases in CMIP SST responses could likewise contribute to differences between observed and CMIP simulated regional climate anomalies (Shin and Sardeshmukh 2011).

Yet, while acknowledging the validity of these various concerns, analysis of the time-evolving summertime surface temperature trends over Texas based on various data sets (Fig. 12) suggests that our initial estimate of a roughly +0.6°C human-induced

warming contribution to 2011 conditions (relative to a 1981-2010 reference) based on CMIP5 data alone is reasonable. The dark box-whisker plots show the median trend value and the spread among the 20 CMIP5 models for periods as long as 110-yrs (left) and as short as 30-yrs (right), all periods ending in 2010. Green circles denote the observed trends. Warming is observed to emerge in recent decades, and this observed behavior is consistent with an accelerated warming trend found also in the CMIP5 simulations. This is further consistent with an accelerated summertime Texas warming trend in recent decades occurring in the AMIP simulations, shown in the light box-whisker plots based on the 12-member GFS historical runs. These various lines of evidence support a view that the region's summertime temperatures have been warming over the last 30 to 40 year period, in a manner that appears to be consistent both in timing and in magnitude with anthropogenic forcing.

No long-term warming has been observed during summer over Texas for periods of analysis greater than about 50-years, however. Furthermore, there is little consistency between the observed and CMIP5 trends over these longer time scales, with the observed trends often residing outside the range of the 20-model CMIP5 simulations. The true anthropogenic warming signal during summer over Texas that spans the entire 20th Century is thus highly uncertain given the appreciable differences between model and observations, and further research is required to understand the reasons for these discrepancies.

Some have proposed using observational trends calculated only since the 1980s to infer the true human-induced warming rate, with the argument being that the recent decades exhibit the most intense anthropogenic forcing (e.g., Rahmstorf and Coumou 2011). But such an approach risks conflating the true external signal of climate change with natural coupled ocean-atmosphere variability. In the case of Texas, if one were to embrace the observed trend value during 1981-2010 period as an estimate of the human-induced warming, for instance, then the inferred warming would be only half the magnitude of the CMIP5 ensemble mean signal. This could be justified if indeed the trends were strongly deterministic in their relationship with radiative forcing. In such a scenario, the spread among the CMIP5 model trends would be an indication of different model sensitivities (implying biases) to the forcing, while the observed trend would be the true signal of change. However, analysis of trends based on the AMIP realizations indicates that much of the spread in trends, post-1950, is actually due to random variability (see Fig. 12). Since each run of this AMIP ensemble is forced identically by the observed SST, sea ice, and CO_2 variability, and utilizes the same model, the range of trends is solely due to atmospheric noise. Given that the amplitude of this range approximates the range among the 20 CMIP model trends, the latter is thus likely also mainly due to noise, rather than being an expression of different plausible sensitivities to anthropogenic forcing and biases. There is no reason, therefore, to assume that a single observed regional trend is also not a combination of a true signal and an appreciable noise component (e.g. Deser et al. 2012).

Based on the data sets available in this study, the only reliable estimate of the signal due to external forcing is the ensemble mean of all models, rather than any single model run or the observed trend. In this regard, it is important that the CMIP5 and AMIP median Texas warming trends are virtually identical for the 1981-2010 period. Given that the AMIP suite was forced with the actual SSTs, the agreement with CMIP5 implies that aforementioned CMIP model biases in SST simulations were either random across individual models and thus minimized via ensemble averaging, or that the Texas summertime temperature sensitivity to such biases is low. It cannot be discounted entirely that the agreement is in part fortuitous, and that CMIP5 systematic errors in sensitivity to external forcing have opposed the effects of natural oceanic variability. Nonetheless, the agreement of CMIP and AMIP median trends may provide an independent and consistent estimate for the probable magnitude of the human-induced mean warming of Texas summer temperatures.

d. Event Probability

How did various factors operating in 2011 alter the probability of breaking the prior Texas heat wave record? In their diagnosis of the 2003 western European heat wave, Stott et al. (2004) developed a procedure for estimating how human-induced climate change affected the probability of a record event. Here we employ similar methods but broaden the scope to reveal not only how anthropogenic forcing affected event probability, but also how the particular state of 2011 global SSTs affected event probabilities. As in Stott et al. (2004), we attempt to avoid selection

bias by examining the threshold corresponding to the prior observed Texas heat wave magnitude (+1.6°C), rather than the particular 2011 event magnitude (+2.9°C). A threshold of +1.6°C corresponds to about a 2 standard deviation departure (2-sigma) in observations, and is thus also more amenable to sampling using the ensemble sizes that are available to this study. For precipitation we select a threshold of -50% departure, for which there had been 4 prior summertime event occurrences at least as dry in the 1895-2010 observational record (Fig. 5), though this threshold is considerably less than the -70% departure during summer 2011.

The results for precipitation are summarized in Table 2 which suggest a vastly different effect of anthropogenic greenhouse gas forcing versus the 2011 SST forcing on the likelihood of extreme drought. The CMIP5 projections indicate no material change in the dry event probability relative to 1981-2010. The AMIP simulations indicate a near 4-fold increase in event threshold exceedence, with an expected return time of 11 years during 1981-2011 becoming only about 3 years under the influence of 2011 SST states. We interpret this result as revealing mainly the strong La Niña effect on the southern Plains rainfall identified in numerous previous observational and modeling studies. The apparent lack of a dry tail sensitivity in CMIP5 projections appears consistent with an overall lack of a mean rainfall change. It is interesting to note, however, that the CMIP5 projections suggest an increase in the probability of extreme wet summer seasons during 2011 (see Fig. 7). In contrast, the 2011 SST patterns severely reduce the probability of an extreme wet Texas summer, while simultaneously enhancing the probability of

severe drought.

Table 3 shows how the probability of exceeding a 2-sigma heat wave threshold had changed in 2011. The absolute value of the threshold varies somewhat among the model simulations because their different standard deviations for temperature (whereas rainfall standardized departures were more similar). The table indicates that while anthropogenic forcing likely increased the probability of a heat wave eclipsing a prior record value (from 5% to 7%), the event probability was increased much more by the particular global SST conditions occurring in 2011. In the AMIP runs, the probability of exceeding a 2-sigma heat wave is estimated at 24% during summer 2011, compared to only a 4% probability during 1981-2010. The AMIP runs present a consistent picture for the joint change in extreme drought and heat wave probabilities with both conditions greatly increasing their probabilities in 2011, physically consistent with the known strong influence of dryness on summertime temperature (e.g. Mueller and Senevirante 2012). By comparison, the CMIP5 simulations reveal a different physical process operating. The effects of greenhouse gas and aerosol forcing act to increase summertime temperatures through radiative processes while not materially altering mean precipitation and thus not initiating the strong surface energy balance responses and feedbacks that lead to heat waves during droughts as occurred in 2011.

The current analysis has been conducted with respect to a 1981-2010 reference, and in this sense all of the changes in probabilities can be meaningfully inter-compared among various model simulations. One might, nonetheless, raise the

more general question of how anthropogenic forcing has changed the event probability in 2011, but relative to an earlier reference frame such as pre-industrial climate. We address this question further in section 4. Here it is important to recognize the difficulty in interpreting the meaning of such analysis given the lack of an overall century-scale temperature trend over Texas. While our analysis supports a view that most of the potential summertime Texas warming due to human influences has likely emerged after 1980, there are large discrepancies between CMIP and observed warming trends over longer periods.

e. Predictability

How predictable was the extreme event of 2011, and can our scientific understanding of the causes for this extreme event be utilized to improve the effectiveness of societal responses via early warnings (e.g. Lubchenco and Karl 2012)? The results from the NOAA/NCEP operational prediction systems are shown in Fig. 13. These predictions warned in advance that Texas --- more so than any other region over the U.S. in summer 2011--- was especially prone to having a hot/dry summer as a consequence of the particular meteorological, oceanic, and soil moisture settings in May 2011 from which each forecast system was initialized. Nonetheless, the distributions of model realizations still affirms the rare and highly unlikely outcome that was observed over Texas, even when the prediction systems were constrained by observations as near to the event as May 2011. The predicted mean temperature anomalies averaged for Texas were +0.7°C and +0.8°C and the mean predicted precipitation departures were -22% and -9%, for CFSv1 and CFSv2,

respectively. CFSv2 forecasts begun even earlier, based on April 2011 initializations, also consistently predicted elevated summer temperatures across the southern Great Plains (Luo and Zhang 2012).

While recognizing the rarity of 2011 event occurrences within the ensemble of CFS predictions, the changes in probability of exceeding prior record values was greatly elevated in both systems relative to their event frequencies in the hindcast period. Based on analysis of the PDFs in Fig. 13, Table 2 summarizes the estimated frequencies and return periods for summer rainfall less than 50% of the models' climatological rainfall (note from Fig. 5 that four such occurrences were observed during 1895-2011). The event likelihood in 2011 predictions roughly doubled, and an event of this intensity is estimated to have an 8-year return period for the 2011 initialized conditions compared to a 20-yr return period during the hindcast period of 1981-2010. For a heat wave magnitude threshold roughly equal to the prior observed Texas summertime record, the predicted probability for 2011 more than tripled relative to the overall probability in the hindcast period.

A more detailed analysis of the dynamical predictions will be the subject of a separate study, though a few additional features of the predictions are worthy of mention here. First, the magnitude of summer rainfall departures is more than twice as large in CFSv1 compared to CFSv2, yet the two predictions produce similar mean warming over Texas. While recognizing numerous fundamental differences in these models which could have bearing on Texas climate variability, one notable

difference is that CFSv2 includes time varying CO_2 and thus includes a factor contributing to warming that is absent in CFSv1. Second, although both prediction systems were initialized with the May 2011 soil moisture conditions, and thus in principle incorporated the full intensity of the cumulative antecedent observed drought, the uninitialized AMIP simulations (using GFSv2) yield warmer and drier summer conditions. Reasons for this difference are not entirely known, although substantial errors in the CFS SST forecasts for June-August (not shown) appear to have forfeited some SST impacts on the summertime Texas extremes that were incorporated in the AMIP forcing with observed SSTs. Finally, no formal verification of the predicted changes in extreme event thresholds has been presented herein, and indeed such an undertaking will be difficult given the rare nature of such extreme events. In the interim, large multi-model approaches will be essential that can provide some indication of confidence and uncertainty based on model reproducibility.

4. Summary and Concluding Remarks

Through a physically-based analysis of observations and climate models, this study sought to identify the causes for and the predictability of the extreme U.S. drought and heat wave of 2011, whose epicenter was Texas but whose extent consumed adjacent Southern Plains states as well. Placing the event within a climatological context revealed no appreciable century-long change in summer temperature and an increase in rainfall over Texas. Thus, no strong evidence for a detected change toward either hotter or drier summers was found for Texas specifically, consistent

with prior studies revealing the central and southern U.S. to be a "warming hole" region overall (Kunkel et al. 2006; Groisman et al. 2012). Our study demonstrated that the principal physical process contributing to the record setting heat wave magnitude was the occurrence of a commensurate extreme precipitation deficit, both during the preceding winter/spring, and continuing during summer 2011. Our diagnosis of climate simulations further confirmed that the probability of record setting summer temperatures over Texas in 2011 was considerably elevated by the condition of antecedent rainfall deficits (dry soils), consistent with empirical studies on shifts in probabilities for hot summers conditioned by precipitation deficits (Hirschi et al. 2011; Mueller and Senevirante 2012).

The paper addressed the underlying causes for the precipitation deficits, demonstrating from diagnosis of AMIP simulations that much of the antecedent and summer precipitation deficits were reconcilable with the region's sensitivity to the particular global SST patterns during 2011. Various lines of evidence indicated that the drought-producing SST forcing was primarily associated with a naturally varying state of the oceans, especially related to La Niña conditions consisting of a cold tropical east Pacific Ocean to which numerous prior observational modeling studies have shown strong southern Plains rainfall sensitivity. Analysis of AMIP simulations also revealed a 4-fold increase in the 2011 probability (relative to chances during 1981-2010) that Texas summertime rainfall would be lower than 50% of normal. In contrast, our diagnosis of CMIP5 projections for 2011 revealed no change in either seasonal mean Texas rainfall or the probability of extreme dry

threshold exceedences, indicating that the drought, and the appreciable fraction of observed summer heat attributed to the dryness, was primarily unrelated to anthropogenic climate change. About 80% (2.3°C) of the observed 2011 Texas heat wave magnitude of 2.9°C was estimated to have resulted from natural variability, principally through physical processes associated with the severe rainfall deficits. About 0.6°C (20%) of the heat wave magnitude relative to 1981-2010 mean was estimated to be attributable to human-induced climate change, based on analysis of time-evolving summertime surface temperature trends over Texas in observational and various model data.

Diagnosis of seasonal forecast systems revealed that much of the regional pattern and an appreciable fraction of the magnitude of both the summertime Texas rainfall deficits and heat wave were predictable from May 2011 initializations. These predictions for 2011 indicated appreciably elevated probabilities of exceeding prior record heat wave and severe drought thresholds relative to the hindcast period of 1981-2010. They captured much of the change in event probabilities identified in the retrospective AMIP simulations which were uninitialized, but were forced with the actual observed ocean conditions.

This attribution study had a purpose and goal considerably broader than just an assessment of the role of overall human-induced climate change, and examined causes more generally with a goal to advance predictive understanding. Thus, to the extent that natural variability played a key role in the extreme event (as it did in

2011), we attempted to reconcile the characteristics and features of the underlying natural processes with a capacity to predict their evolution and impacts. To this end, we analyzed initialized coupled forecast systems that were part of NOAA's operational seasonal forecasting activities, the diagnosis of which was complemented by a study of uninitialized CMIP5 simulations. The use of a recent 30-year reference period is standard procedure for expressing forecast anomalies in operational seasonal prediction practices, and is also the standard WMO guideline for diagnosing seasonal climate anomalies in routine monitoring practices. Yet, the more narrow question of the attributable effect of overall human-induced climate change since pre-industrial times is clearly also of interest.

We have conducted an additional analysis of CMIP5 simulations to assess how extreme heat wave event probabilities for pre-industrial climate conditions changed in those same models but under the influence of external radiative conditions circa 2011. We determined that the mean summertime temperature increase relative to pre-industrial conditions is +1.2°C from such an analysis, double the estimated warming relative to 1981-2010. Using a generalized extreme value (GEV) fit to the histogram of model simulations (not shown), a Texas heat wave magnitude equal to 2011 observations (2.9°C) is found to have roughly a 250-yr return period in these pre-industrial climate simulations, whereas such an event is found to have a 10-year return period for 2011. There are various difficulties in interpreting such an analysis and assessing its relevance to understanding observations. First, no summertime warming over Texas in the long historical record has been detected, and we emphasized in this paper that the CMIP5 model simulated Texas warming

over the last century is inconsistent with observations. In the absence of a detected warming over the long record, and in light of the uncertainty in the magnitude of climate change in this region based on CMIP5 experiments, these estimates of changes in event probability drawn solely from CMIP5 must be viewed with great caution. Second, the CMIP5 models have considerably greater summertime temperature variability over Texas than is observed, with the consequence that greater event probabilities for temperature thresholds are estimated from the models than likely exist in nature. To illustrate the considerable sensitivity of these probabilities to exceedence thresholds used, we repeated the above analysis using the observed standardized departure for 2011 (roughly 4 sigma, or 5°C for model equivalent values), rather than employing the observed heat wave of 2.9°C as the threshold. The GEV analysis of model simulations for 2011 then implies a roughly 350-yr return period, far different from the approximately 10-yr return period estimated when using the observe heat wave magnitude as threshold value. In this latter analysis based on standardized departures, one would draw the conclusion that a heat wave event of the intensity of 2011 was indeed a very rare occurrence.

Ultimately, the question of greatest concern is whether a drought/heat wave as severe as occurred over Texas in 2011 can be anticipated. Our results have some implication for addressing such a concern. First, the results of this analysis provide evidence for a considerable seasonal predictability of an event of the type observed during 2011 owing to the impact of slow modes of ocean variability associated with the El Niño/La Niña phenomenon (and perhaps also Atlantic SSTs). As such, a capability for useful early warning several seasons in advance exists. Second, our

analysis reveals that intrinsic variability of the atmosphere alone has the capacity to generate drought and heat waves of considerable magnitude and was important in determining the ultimate magnitude of this event. There is currently very limited predictability of such atmospheric driven extremes at lead times beyond the time scale of useful weather predictability of about 2 weeks. And, finally regarding the possible impacts of human-induced climate change and its connection with anticipating the 2011 event, several specific science challenges for the region of the Southern Plains remain. In particular, there is a need for a complete and physically-based explanation for why there has been a lack of overall warming during the last century over this region; providing reasons for the overall increase in rainfall would be key to understanding such a lack of warming.

Acknowledgments. The authors thank Mike Wehner and three additional, anonymous reviewers for their helpful reviews of the manuscript. NCAR provided some of the data for the CCSM4 simulations. We acknowledge the World Climate Research Program's Working Group on Coupled Modelling, which is responsible for CMIP, and we thank the climate modeling groups for producing and making available their model output. For CMIP the U.S. Department of Energy's Program for Climate Model Diagnosis and Intercomparison provides coordinating support and led development of software infrastructure in partnership with the Global Organization for Earth System Science Portals.

References

Compo, G. P., and P. D. Sardeshmukh, 2009: Oceanic influences on recent continental warming. *Climate Dyn*., **32**, 333–342, doi:10.1007/s00382-008 0448-9.

Deser, C., R. Knutti, S. Solomon, and A. S. Phillips, 2012: Communication of the role of natural variability in future North American climate. *Nature Clim. Change*, (accepted).

Dole, R, M. Hoerling, J. Perlwitz, J. Eischeid, P. Pegion, TZhang, X. Quan, T. Xu, and D. Murray; 2011: Was there a basis for anticipating the 2010 Russian heat wave? *Geophys. Res. Lett,,* **3**8, L06702, doi:10.1029/2010GL046582.

Dommenget, D., 2009: The ocean's role in continental climate variability and change. *J. Climate,* **22**, 4939–4952.

Fischer, E., and C. Schar, 2010: Consistent geographical patterns of changes in high-impact European heatwaves. *Nature Geosci.,* **3**, 398-403.

Fannin, B., 2012: Updated 2011 Texas agricultural drought losses total $7.62 billion. AgriLife TODAY, http://today.agrilife.org/2012/03/21/updated-

2011-texas-agricultural-drought-losses-total-7-62-billion/, accessed April 22, 2012.

Findell, Kirsten L., Thomas L. Delworth, 2010: Impact of Common Sea Surface Temperature Anomalies on Global Drought and Pluvial Frequency. *J. Climate*, **23**, 485–503.

Gent, Peter R., and Coauthors, 2011: The Community Climate System Model Version 4. *J. Climate*, **24**, 4973-4991. doi:,http://dx.doi.org/10.1175/2011JCLI4083.1

Greenberg, J. H., J. Bromberg, C. M. Reed, T. L. Gustafson, and R. A. Beauchamp, 1983: The epidemiology of heat-related deaths, Texas – 1950, 1970-79, and 1980. *Amer. J. Public Health*, **73**, 805-807.

Groisman, Pavel Ya., Richard W. Knight, Thomas R. Karl, 2012: Changes in Intense Precipitation over the Central United States. *J. Hydrometeor*, **13**, 47–66.

Guttman, N. B., and R. G. Quayle, 1996: A historical perspective of U.S. climate divisions. *Bull. Amer. Meteor. Soc.*, **77**, 293-303.

Hirschi, M, and Co-Authors, 2011: Observational evidence for soil-moisture impact on hot extremes in southeastern Europe. *Nature Geo.*, **4**, 17-21.

Hoerling, M., T. Xu, G. Bates, A. Kumar, and B. Jha, 2006: Warm oceans raise land temperatures. *Eos*, Trans. Amer. Geophys. Union, **87**, doi:10.1029/2006EO190003.

Hoerling, M., A. Kumar, J. Eischeid, and B. Jha, 2008: What is causing the variability in global mean land temperature. *Geophys. Res. Lett.*, **35**, L23712, doi:10.1029/2008GL035984.

Hoerling, M., X. Quan, and J. Eischeid (2009), Distinct causes for two principal U.S. droughts of the 20th century, *Geophys. Res. Lett.*, **36**, L19708, doi:10.1029/2009GL039860.

Hoerling, M., J. Eischeid, and J. Perlwitz, 2010: Regional precipitation trends: Distinguishing natural variability from anthropogenic forcing. *J. Climate*, **23**, 2131-2145.

Hoerling, M., J. Eischeid, J. Perlwitz, X. Quan, T. Zhang, and P. Pegion, 2012: On the increased frequency of Mediterranean drought. *J. Climate*, **25**, 2146-2161.

Hong, S.-Y., and E. Kalnay, 2000: Role of sea surface temperature and soil-moisture in the 1988 Oklahoma-Texas drought. *Nature*, **408**, 842-844.

Hong, S.-Y., and E. Kalnay, 2002: The 1988 Oklahoma –Texas drought: Mechanistic experiments with NCEP global and regional models. *J. Climate*, **15**, 945-963.

IPCC, 2012: *Managing the Risks of Extreme Events and Disasters to Advance Climate Change Adaptation.* A Special Report of Working Groups I and II of the Intergovernmental Panel on Climate Change [Field, C.B., V. Barros, T.F. Stocker, D. Qin, D.J. Dokken, K.L. Ebi, M.D. Mastrandrea, K.J. Mach, G.-K. Plattner, S.K. Allen, M. Tignor, and P.M. Midgley (eds.)]. Cambridge University Press, Cambridge, UK, and New York, NY, USA, 582 pp.

Jones, G. S., Stott, P. A., Christidis, N., 2008: Human contribution to rapidly increasing frequency of very warm Northern hemisphere summers. *J. Geophys. Res.*, **113**, D02109, doi:10.1029/2007JD008914.

Kiladis, G., and H. Diaz, 1989: Global climatic anomalies associated with extreme phases in the Southern Oscillation. *J. Climate*, **2**, 1069-1090.

Knutson, T., and Coauthors, 2006: Assessment of twentieth-century regional surface temperature trends using the GFDL CM2 coupled models. *J. Climate*, **19**, 1624–1651.

Koster, R., and Co-Authors, 2004: Regions of strong coupling between soil moisture and precipitation. *Science*, **305**, 1138-1140

Krakauer, N., B. Cook, and M. Puma, 2010: Contribution of soil moisture feedback to hydroclimatic variability. *Hydrol. Syst. Sci,* **14**, 505-520.

Kunkel, K., X. Liang, J. Zhu, and Y. Lin, 2006: Can CGCMs simulate the Twentieth-Century "Warming Hole" in the Central United States?. *J. Climate*, **19**, 4137-4153.

Lawrence, Peter J., and Coauthors, 2012: Simulating the Biogeochemical and Biogeophysical Impacts of Transient Land Cover Change and Wood Harvest in the Community Climate System Model (CCSM4) from 1850 to 2100. *J. Climate*, **25**, 3071–3095.

Leibensperger, E. M., Mickley, L. J., Jacob, D. J., Chen, W.-T., Seinfeld, J. H., Nenes, A., Adams, P. J., Streets, D. G., Kumar, N., and Rind, D.: Climatic effects of 1950–2050 changes in US anthropogenic aerosols – Part 2: Climate response, *Atmos. Chem. Phys.*, **12**, 3349-3362, doi:10.5194/acp-12-3349-2012, 2012.

Lubchenco, J. and T. R. Karl, 2012: Predicting and managing extreme weather events. *Physics Today*, **65**, 31-31.

Luo, L. and Y. Zhang (2012), Did We See the 2011 Summer Heat Wave

Coming?, *Geophys. Res. Lett.*, doi:10.1029/2012GL051383

Lyon, B., and R. M. Dole, 1995: A diagnostic comparison of the 1980 and 1988 U.S. summer heat wave-droughts. *J. Climate*, **8**, 1658–1675.

Madden, R., and J. Williams, 1978: The correlation between temperature and precipitation in the United States and Europe. *Mon. Wea. Rev.*, **106**, 142-147.

McRoberts, D. Brent, John W. Nielsen-Gammon, 2011: A New Homogenized Climate Division Precipitation Dataset for Analysis of Climate Variability and Climate Change. *J. Appl. Meteor. Climatol.*, **50**, 1187–1199.

Meehl, G. A., C. Tebaldi, G. Walton, D. Easterling, and L. McDaniel (2009), Relative increase of record high maximum temperatures compared to record low minimum temperatures in the U.S., *Geophys. Res. Lett.*, ***36***, L23701, doi:10.1029/2009GL040736.

Moss, R. H., J. A. Edmonds, K. A. Hibbard, M. R. Manning, S. K. Rose, D. P. van Vuuren, T. R. Carter, S. Emori, M. Kainuma, T. Kram, G. Meehl, J. F. B. Mitchell, N. Nakicenovic, K. Riahi, S. J. Smith, R. J. Stouffer, A. M. Thomson, J. P. Weyant, T. J. Wilbanks, 2010: The next generation of scenarios for climate change research and assessment. *Nature*, **463**, 747-756.

Mueller, B. and S. Seneviratne, 2012: Hot days induced by precipitation deficits at the global scale, *Proc. National Academy of Sciences*, **109**, 12398-12403

Namias, J., 1982: Anatomy of Great Plains protracted heat waves (especially the 1980 U.S. summer drought). *Mon. Wea. Rev*., **110**, 824-838.

NCDC (National Climate Data Center), 2002: Time bias corrected divisional temperature-precipitation-drought index. Documentation for dataset TD-9640. National Climatic Data Center, Asheville, NC, 12 pp. Report available at http://www1.ncdc.noaa.gov/pub/data/documentlibrary/tddoc/td9640.pdf

Pan, Z., R. W. Arritt, E. S. Takle, W. J. Gutowski Jr., C. J. Anderson, and M. Segal, 2004: Altered hydrologic feedback in a warming climate introduces a "warming hole." *Geophys. Res. Lett.,* **31,** L17109, doi:10.1029/2004GL020528.

Rahmstorf, S., and D. Coumou, 2011: Increase of extreme events in a warming world. *Proc. Nat. Acad. Sci*., doi: 10.1073/pnas.1101766108

Rayner, N. A.; Parker, D. E.; Horton, E. B.; Folland, C. K.; Alexander, L. V.; Rowell, D. P.; Kent, E. C.; Kaplan, A. (2003) Global analyses of sea surface temperature, sea ice, and night marine air temperature since the late

nineteenth century *J. Geophys. Res*.**, 108**, No. D14, 4407 10.1029/2002JD002670

Saha, S., S. Nadiga, C. Thiaw, J. Wang, Q. Zhang, H.M. van de Dool, H.-.L.Pan, S. Moorthi, D. Behringer, D. Stokes, M.Pena, S. Lord, G. White, W. Ebisuzaki, P. Peng, and P. Xie, 2006: The NCEP Climate Forecast System. *J. Climate*, **19**, 3483-3517.

Schubert, S.D., M. J. Suarez, P. J. Pegion, R. D. Koster, and J. T. Bacmeister , 2004a: On the Cause of the 1930s Dust Bowl, *Science,* **33**, 1855-1859.

Schubert, S.D., M. J. Suarez, P. J. Pegion, R. D. Koster, and J. T. Bacmeister , 2004b: Causes of long-term drought in the United States Great Plains. *J. Climate*., **17**, 485-503.

Schubert, S.D., and Co-Authors, 2009: A U.S. CLIVAR Project to assess and compare the responses of global climate models to drought-related SST forcing patterns: Overview and results. *J. Climate*, **22**, 5251-5272.

Seager, R., Y. Kushnir, C. Herweijer, N. Naik, and J. Velez, 2005: Modeling the tropicalforcing of persistent droughts and pluvials over western North America: 1856-2000. *J. Climate*., **18**, 4068-4091.

Senevirante, S. I., D. Luthi, M. Litschi, and C. Schar, 2006: Land-atmosphere coupling and climate change in Europe. *Nature*, **443**, 205-209.

Shin, S., and P. Sardeshmukh, 2011: Critical influence of the pattern of tropical ocean warming in remote climate trends. *Clim. Dyn.*, **36**, 1577-1591.

Stott, P. A., Stone, D. A., Allen, M. R., 2004: Human contribution to the European heatwave of 2003. *Nature*, **432**, 610-614.

Taylor, K. E., R. J. Stouffer, and G. A. Meehl, 2012: The CMIP5 Experiment Design. *Bull. Amer. Meteorol. Soc.*, in review. (A summary of the CMIP5 Experimental Design is available at http://cmip-pcmdi.llnl.gov/cmip5/docs/Taylor_CMIP5_design.pdf.

Texas Forest Service, 2012: Preliminary estimation of drought economic loss in East Texasforests. Report available at http://texasforestservice.tamu.edu/uploadedFiles/FRD/Economic_Loss_of_East_Texas_Forests_from_the_Drought.pdf, accessed April 22, 2012

Ting, M., Y. Kushnir, R. Seager, and C. Li., 2009: Forced and internal Twentieth Century SST trends in the North Atlantic. *J. Climate*, **22**, 1469-1481.

Wang, Hailan, Siegfried Schubert, Max Suarez, Junye Chen, Martin Hoerling, Arun Kumar, Philip Pegion, 2009: Attribution of the Seasonality and Regionality in Climate Trends over the United States during 1950–2000. *J. Climate*, **22**, 2571–2590.

Figure Captions

Figure 1. The observed 2011 June-August (JJA) averaged surface temperature departures (°C, top), the time series of JJA Texas surface temperature departures (°C, bottom, left), and the probability distribution functions of the JJA Texas surface temperatures for two sub-periods of the historical record: 1895-1954 (blue curve), and 1955-2010 (red curve). The observed 2011 JJA Texas surface temperature shown in gray tick mark. Data source is the NCDC U.S. Climate Divisions, and departures are relative to 1981-2010 means. The PDFs are non-parametric curves constructed using the R software program which utilizes a kernal density estimation and a Guassian smoother.

Figure 2. Histogram of the temperature departures (°C) for the hottest Texas summers occurring in consecutive, non-overlapping 100 year samples of CMIP5 pre-industrial simulations. The block maxima analysis is based on 18 different CMIP5 models, most of which have at least 500-yr long simulations. The prior record observed summertime Texas departure during 1895-2010 indicated by short green tick mark, and the 2011 new record summer departure indicated by long green tick mark. The red PDF is the Gaussian fitted curve to the histogram, while the blue PDF is the non-parametric curve constructed using the R software program which utilizes a kernal density estimation and a Guassian smoother.

Figure 3. The 15-case composite SST (°C, left) and U.S. precipitation anomalies (% of climatology, right) based on the 1 in 100 year hottest summertime Texas heat

wave events occurring in a 1500-yr simulation of CCSM4. The experiment is an unforced, pre-industrial simulation. Top panels show contemporaneous conditions for June-August, and bottom panels show antecedent conditions for October-May. All anomalies are relative to the CCSM4 climatology.

Figure 4. Observed SST anomalies (°C, left) and U.S. precipitation anomalies (% of climatology, right). Top panels show contemporaneous conditions for June-August 2011, and bottom panels show antecedent conditions for October 2010-May 2011. All anomalies are relative to an observed 1981-2010 climatology.

Figure 5. The historical relationship between June-August Texas averaged rainfall departures (% of climatology) and surface temperature departures (°C). Each dot corresponds to a summer during 1895-2010, and the 2011 value is indicated by the blue wagon wheel. Inset values are for the correlation (R) and the slope of the linear fit expressed as °C/%Pcpn departure.

Figure 6. The June-August 2011 U.S. precipitation anomalies (% of climatology, left) and surface temperature anomalies (°C, right). Observed (top), ensemble mean AMIP simulated (middle), and ensemble mean CMIP5 simulated (bottom). The AMIP results are based on an 80-member GFS average for 2011, and the CMIP results are based on a 220-member average using 20 different models for a 11-year window of JJA conditions centered on 2011. All anomalies are relative to the respective data set's 1981-2010 climatology, and the observed scale of plotted anomalies is double

that shown for the simulations. The reference AMIP simulation uses the same GHG concentrations as those specified in the 2011 experiments.

Figure 7. Probability distribution functions of the AMIP (top) and CMIP5 (bottom) simulated summer Texas precipitation anomalies (% of climatology, left) and surface temperature (°C, right). Each panel plots two curves, one for the frequency distribution of simulations during 1981-2010, and the other for the frequency distribution of simulations during 2011. For CMIP5, 600 (220) individual simulations are used for 1981-2010 (2011). For AMIP, 360 (80) individual simulations are used for 1981-2010 (2011). The verical gray tic marks denote the observed 2011 anomalies. All departures are relative to a 1981-2010 reference. The PDFs are non-parametric curves constructed using the R software program which utilizes a kernal density estimation and a Guassian smoother.

Figure 8. The AMIP (top) and CMIP5 (bottom) simulated relationship between June-August Texas averaged rainfall departures (% of climatology) and surface temperature departures (°C). Left (right) panels show the relationship for 1981-2010 (2011). Each dot corresponds to the temperature/precipitation for a particular model realization. For AMIP, there are 360 (80) realizations for 1981-2010 (2011). For CMIP, there are 720 (220) realizations for 1981-2010 (2011). Inset values are for the correlation (R) and the slope (b) of the linear fit expressed as °C/%Pcpn departure. The blue wagon wheel denotes the observed JJA 2011 values.

Figure 9. Observed (red curve) and AMIP ensemble mean (thick black curve) cumulative Texas precipitation departures (mm) from October 20110 through August 2011. Thin black curves are for each of the 80 members of the GFS AMIP simulations. Orange curves are the cumulative precipitation departures for the subset of 8 warmest Texas JJA 2011 GFS realization. Departures are computed relative to the respective data sets' 1981-2010 mean.

Figure 10. The simulated relationship between June-August Texas averaged rainfall departures (% of climatology) and surface temperature departures (°C) for wet (dry) Texas antecedent October-May conditions in green (red) dots. The data is based on the 12-member suite of 1950-2010 GFS AMIP simulations, and the plotted values are for the 10% wettest (driest) October-May realizations corresponding to 72 samples for each extreme.

Figure 11. Probability distribution functions (PDFs) of GFS simulated June-August Texas surface temperature based on a joint condition of dry antecedent and dry summer conditions (red curve), and for unconditional model realizations (blue curve). Red PDF is comprised of the 41 realizations that were among both the driest 20% Oct-May and the driest 20% June-August conditions. Blue PDF is the unconditioned frequency distribution that is comprised of all 720 model realizations. Grey tic mark denotes the magnitude of the observed JJA 2011 Texas temperature departure.

Figure 12. Observed (green dot) and simulated (box/whiskers) trends in June-August Texas surface temperature (°C/decade). Trends are computed for different beginning years from 1901 (left most box) to 1981 (right most boxes), staggered at 10-year increments, while the end year for all trend calculations is 2010 Thus, the longest trend period is for a 110-yr period (left side), and the shortest is for a 30-yr period (right side). Dark (light) box/whiskers display the CMIP5 (AMIP) simulation trends based on a 20-member (12-member) ensemble. The extreme values of the model simulated trends are shown by the red and blue asterikes.

Figure 13. NOAA/NCEP operational dynamical predictions of June-August seasonally averaged precipitation anomalies (% of climatology, left) and surface temperature anomalies (°C, right). Probability distribution functions as in Fig. 7. Spatial anomaly maps as in Fig. 6, except based on the ensemble mean of the CFS forecasts. For CFSv1, 435 (124) individual hindcasts (forecasts) are used for 1981-2009 (2011). For CFSv2, 696 (124) individual hindcasts (forecasts) are used for 1982-2010 (2011). All hindcasts and forecasts are based on initializations from May analyses, and anomalies are calculated relative to the period of available hindcast climatologies for all May initializations

Table 1. Summary of the climate simulations, predictions, and projections diagnosed in the current paper, including the nature of their external and boundary forcings, the length of integrations, and the available ensemble size.

Type	**Model**	**Radiative Forcing**	**SST, Sea Ice**	**Duration** (Target time)	**Ensemble Members**
Pre-industrial simulation	CMIP5	Pre-industrial	Coupled	≥ 500 years	1 run each for 18 models
Historical simulation	GFSv2	Observed CO_2	Observed (AMIP)	1950-2010	12
Event simulation	GFSv2*	Observed CO_2	Observed (AMIP)	Oct. 2009 – Sep. 2011	80
Historical simulation	CMIP5	Observed (see text)	Coupled	1880-2005	1 run each for 20 models
Projection	CMIP5	RCP 4.5 (see text)	Coupled	2006-2016	1 run each for 20 models
Forecast (0-lead)	CFSv1	1988 CO_2	Coupled	June 01 – August 31, 2011	120(initialized every 6 hours)
Hindcast (0-lead)	CFSv1	1988 CO_2	Coupled	June 01 - August 31, 1981-2009	15 (initialized once daily, staggered every 2 days)
Forecast (0-lead)	CFSv2	Observed & projected CO_2	Coupled	June 01 – August 31, 2011	120(initialized every 6 hours)
Hindcast (0-lead)	CFSv2	Observed CO_2	Coupled	June 01 – August 31, 1982-2010	24 (initialized every 6 hours, staggered every 5 days)

* Anomaly calculated relative to a 1981-2010 GFSv2 AMIP set having same CO_2 as the 2011 runs.

Table 2. The left column shows the simulated June-August 2011 Texas precipitation anomalies for the indicated suite of models based on their ensemble average 2011 simulations relative to a 1981-2010 model reference. The standard deviation of simulated June-August surface temperatures is the average of the 1981-2010 runs and the 2011 runs. Event probability and return period in the third column is for the exceedence of a less than 50% of normal precipitation deficit. Event probabilities and return periods in the fourth column are for exceeding this same threshold, but based on the distribution of simulations for 2011. The probabilities are calculated from the non-parametric curves of the simulated frequency distributions shown in the Fig. 7 for CMIP and AMIP, and Fig. 13 for CFS.

MODEL	JJA 2011 TEXAS P_{ANOM}	MODEL STD DEV	EVENT PROBABILITY (1981-2010) RETURN PERIOD	EVENT PROBABILITY (2011) RETURN PERIOD
CMIP5	+0.2%	36.8%	6% 17yr	6% 17yr
AMIP	-33.9%	36.3%	9% 11yr	34% 3yr
CFSv1	-21.5%	36.1%	7% 14yr	16% 6yr
CFSv2	-9.1%	33.4%	5% 20yr	12% 8yr

Table 3. The left column shows the simulated June-August 2011 Texas surface temperature anomalies for the indicated suite of models based on their ensemble average 2011 simulations relative to a 1981-2010 model reference. The standard deviation of simulated June-August surface temperatures is the average of the 1981-2010 runs and the 2011 runs. Event probability and return period in the third column is for the exceedence of a 2 standardized departure warming over Texas for the 1981-2010 distribution of simulations. Event probabilities and return periods in the fourth column are for exceeding this same threshold, but based on the distribution of simulations for 2011. The probabilities are calculated from the non-parametric curves of the simulated frequency distributions shown in the Fig. 7 for CMIP and AMIP, and Fig. 13 for CFS.

MODEL	JJA 2011 TEXAS P_{ANOM}	MODEL STD DEV	EVENT PROBABILITY (1981-2010) RETURN PERIOD	EVENT PROBABILITY (2011) RETURN PERIOD
CMIP5	+0.6°C	1.2°C	3% 33yr	6% 17yr
AMIP	+1.1°C	0.9°C	4% 25yr	23% 4yr
CFSv1	+0.7°C	0.8°C	3% 33yr	10% 10yr
CFSv2	+0.8°C	0.7°C	2% 50yr	17% 6yr

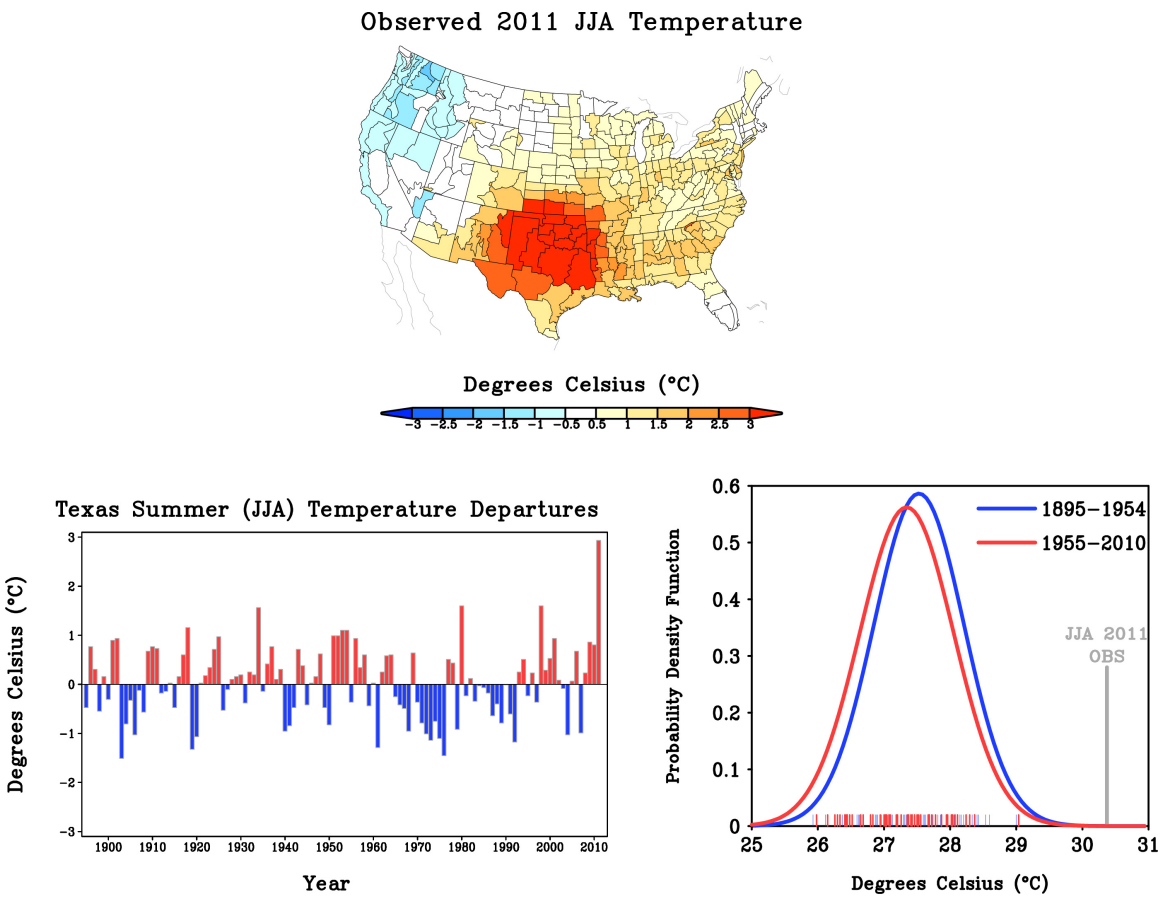

Figure 1. The observed 2011 June-August (JJA) averaged surface temperature departures (°C, top), the time series of JJA Texas surface temperature departures (°C, bottom, left), and the probability distribution functions of the JJA Texas surface temperatures for two sub-periods of the historical record: 1895-1954 (blue curve), and 1955-2010 (red curve). The observed 2011 JJA Texas surface temperature shown in gray tick mark. Data source is the NCDC U.S. Climate Divisions, and departures are relative to 1981-2010 means. The PDFs are non-parametric curves constructed using the R software program which utilizes a kernal density estimation and a Guassian smoother.

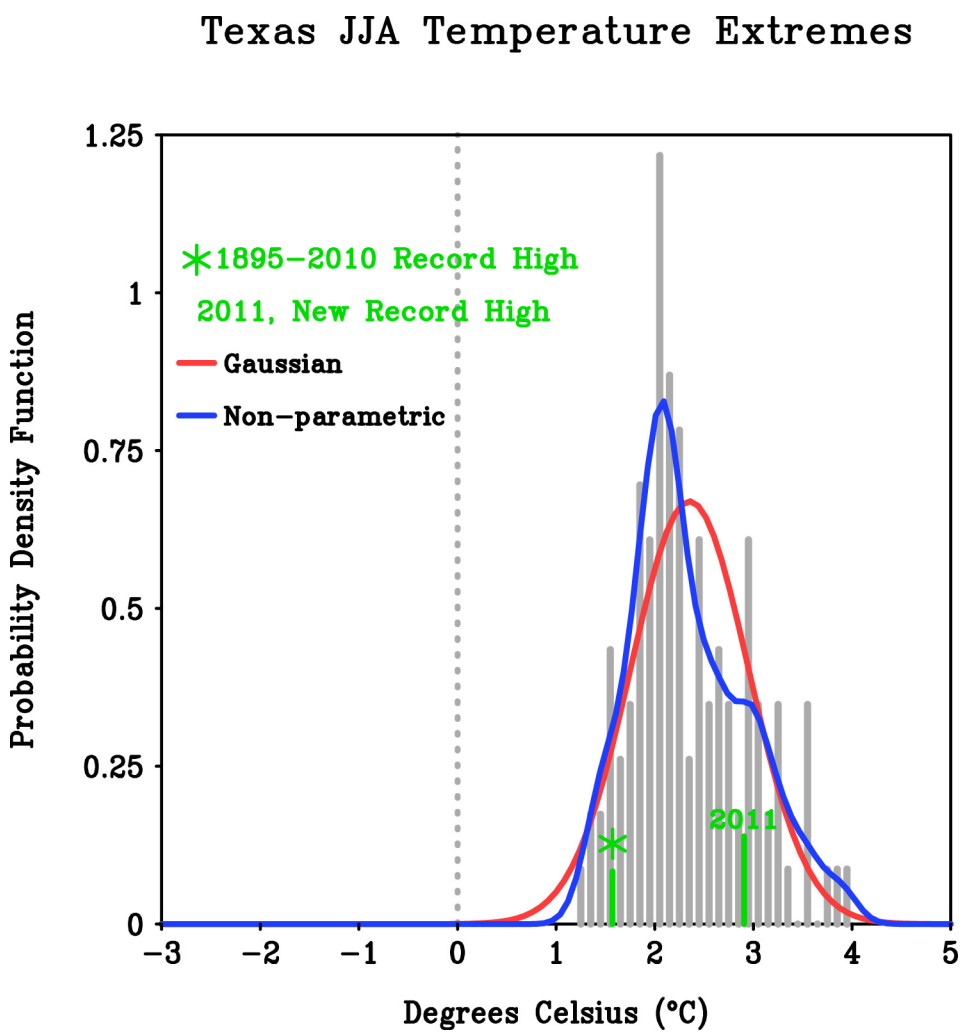

Figure 2. Histogram of the temperature departures (°C) for the hottest Texas summers occurring in consecutive, non-overlapping 100 year samples of CMIP5 pre-industrial simulations. The block maxima analysis is based on 18 different CMIP5 models, most of which have at least 500-yr long simulations. The prior record observed summertime Texas departure during 1895-2010 indicated by short green tick mark, and the 2011 new record summer departure indicated by long green tick mark. The red PDF is the Gaussian fitted curve to the histogram, while the blue PDF is the non-parametric curve constructed using the R software program which utilizes a kernal density estimation and a Guassian smoother.

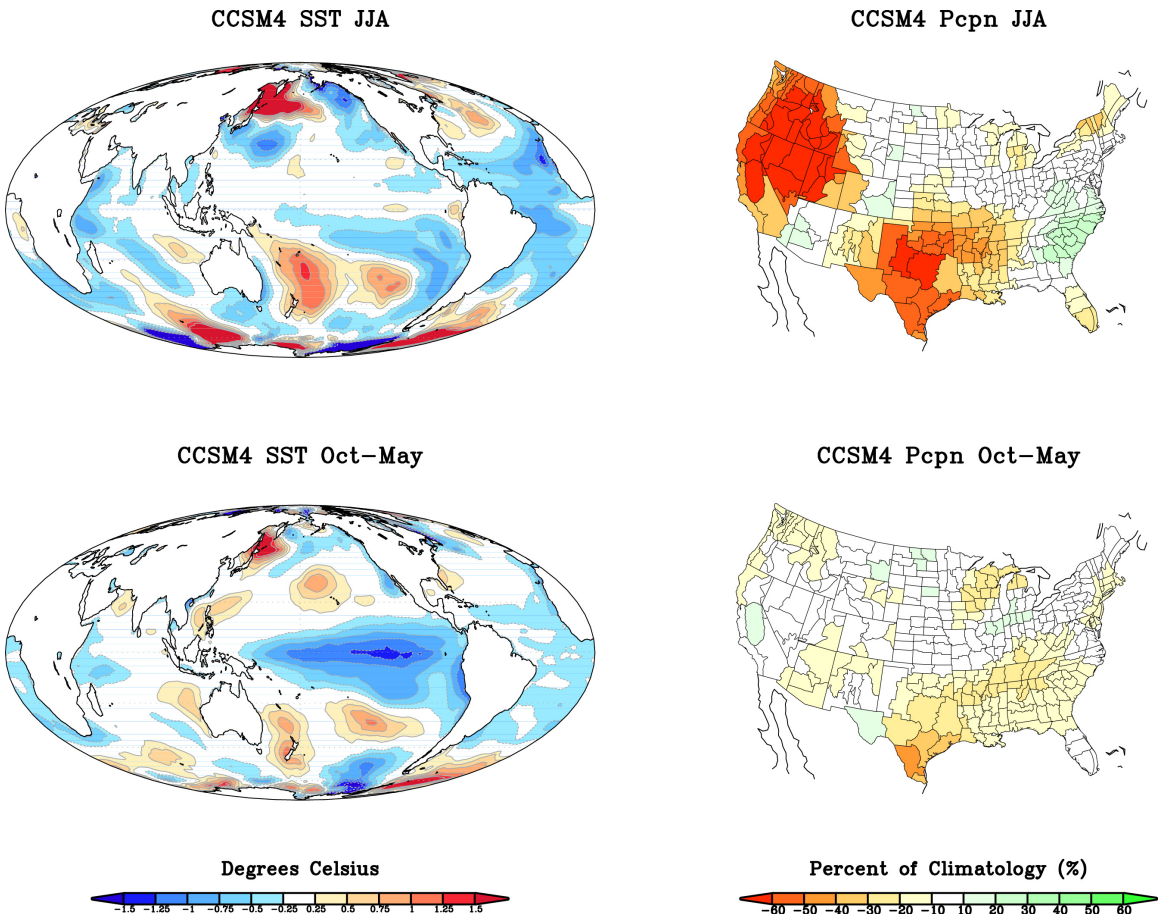

Figure 3. The 15-case composite SST (°C, left) and U.S. precipitation anomalies (% of climatology, right) based on the 1 in 100 year hottest summertime Texas heat wave events occurring in a 1500-yr simulation of CCSM4. The experiment is an unforced, pre-industrial simulation. Top panels show contemporaneous conditions for June-August, and bottom panels show antecedent conditions for October-May. All anomalies are relative to the CCSM4 climatology.

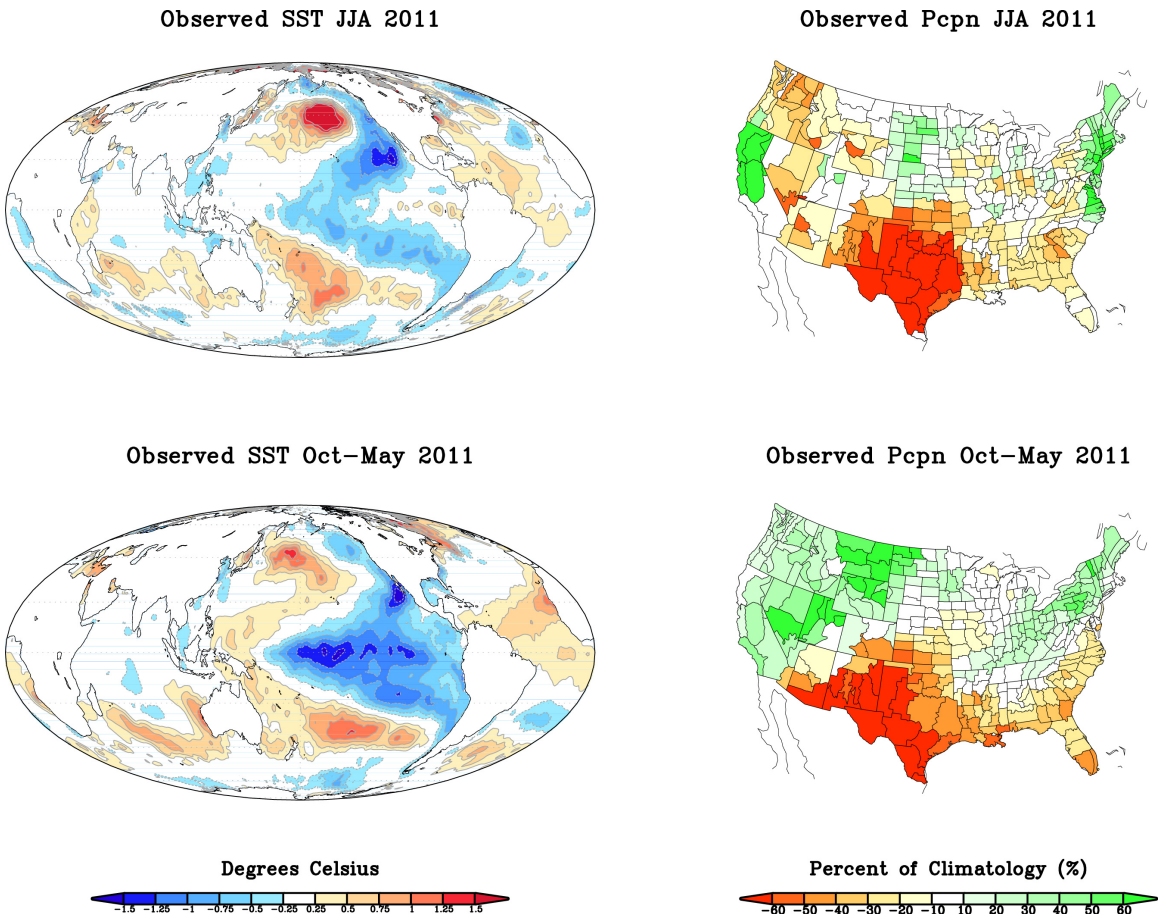

Figure 4. Observed SST anomalies (°C, left) and U.S. precipitation anomalies (% of climatology, right). Top panels show contemporaneous conditions for June-August 2011, and bottom panels show antecedent conditions for October 2010-May 2011. All anomalies are relative to an observed 1981-2010 climatology.

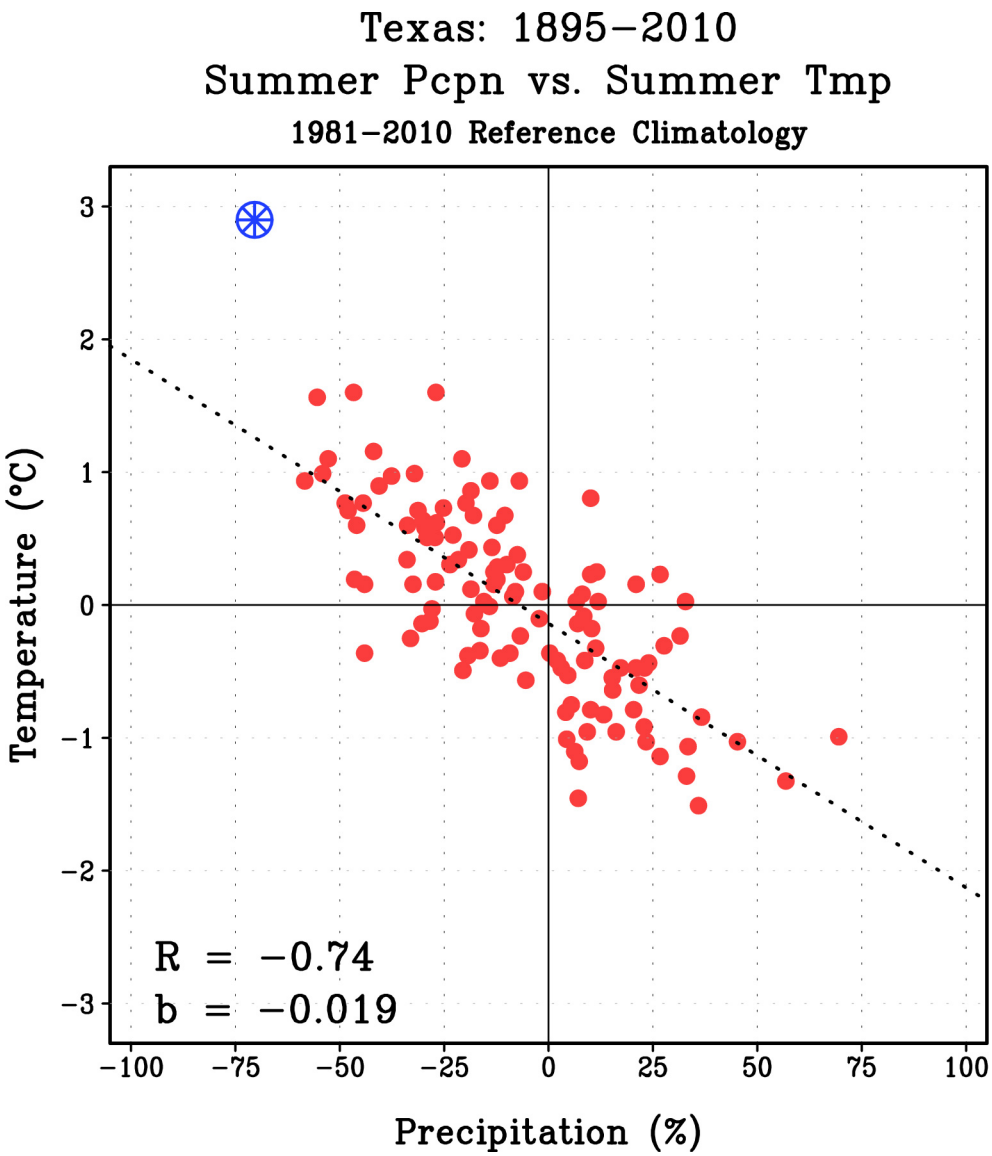

Figure 5. The historical relationship between June-August Texas averaged rainfall departures (% of climatology) and surface temperature departures (°C). Each dot corresponds to a summer during 1895-2010, and the 2011 value is indicated by the blue wagon wheel. Inset values are for the correlation (R) and the slope of the linear fit expressed as °C/%Pcpn departure.

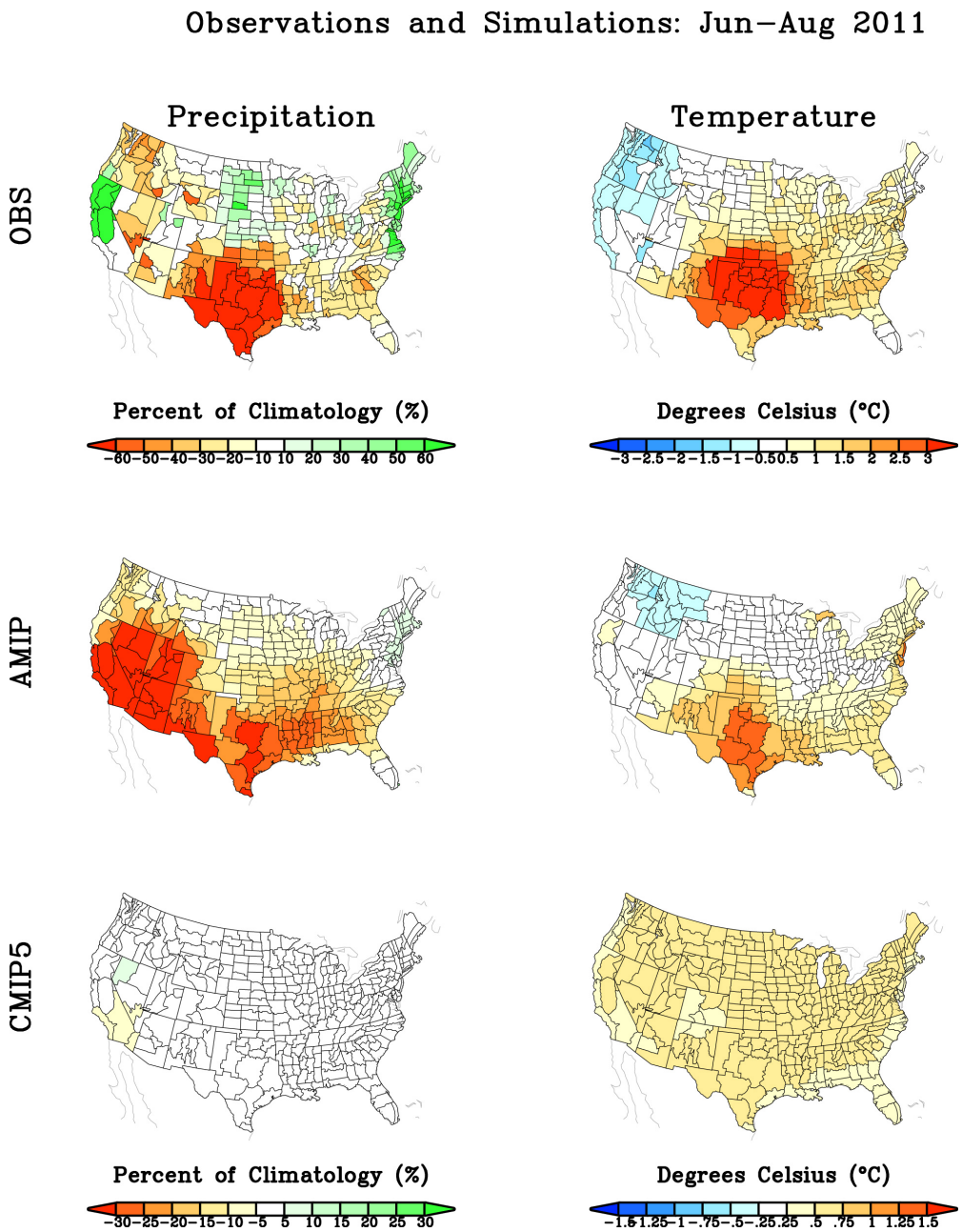

Figure 6. The June-August 2011 U.S. precipitation anomalies (% of climatology, left) and surface temperature anomalies (°C, right). Observed (top), ensemble mean AMIP simulated (middle), and ensemble mean CMIP5 simulated (bottom). The AMIP results are based on an 80-member GFS average for 2011, and the CMIP results are based on a 220-member average using 20 different models for a 11-year window of JJA conditions centered on 2011. All anomalies are relative to the respective data set's 1981-2010 climatology, and the observed scale of plotted anomalies is double that shown for the simulations. The reference AMIP simulation uses the same GHG concentrations as those specified in the 2011 experiments.

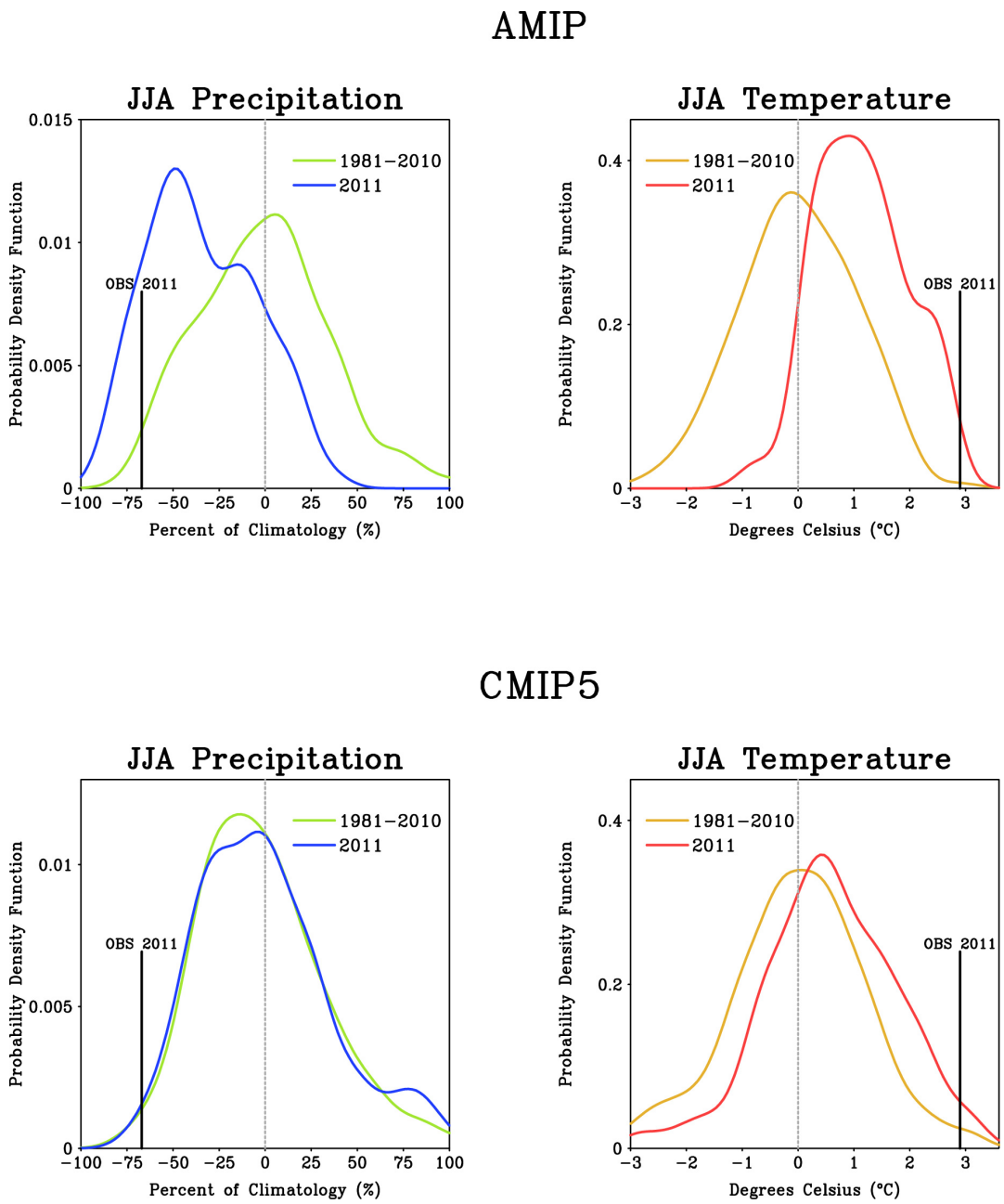

Figure 7. Probability distribution functions of the AMIP (top) and CMIP5 (bottom) simulated summer Texas precipitation anomalies (% of climatology, left) and surface temperature (°C, right). Each panel plots two curves, one for the frequency distribution of simulations during 1981-2010, and the other for the frequency distribution of simulations during 2011. For CMIP5, 600 (220) individual simulations are used for 1981-2010 (2011). For AMIP, 360 (80) individual simulations are used for 1981-2010 (2011). The verical gray tic marks denote the observed 2011 anomalies. All departures are relative to a 1981-2010 reference. The PDFs are non-parametric curves constructed using the R software program which utilizes a kernal density estimation and a Guassian smoother.

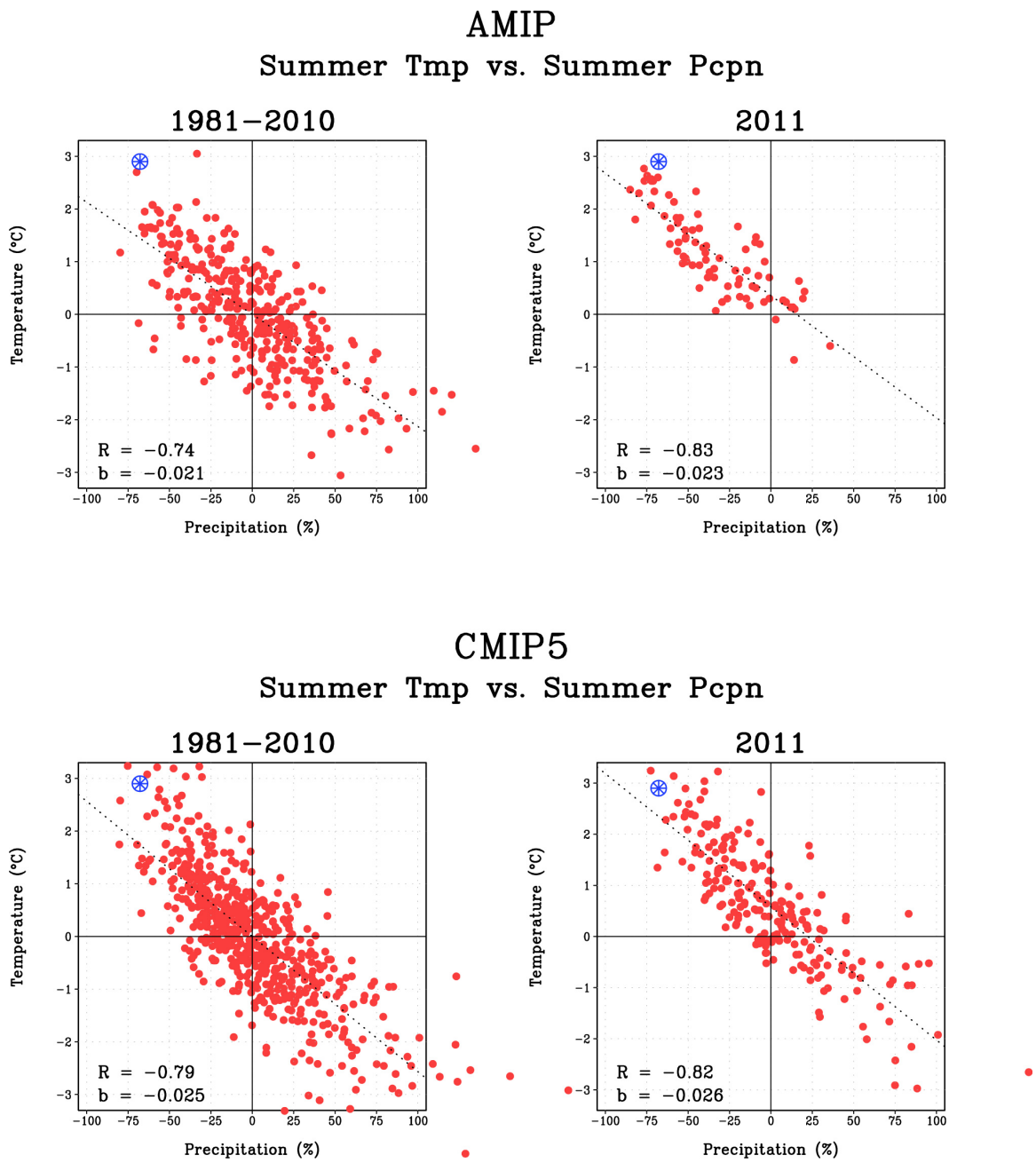

Figure 8. The AMIP (top) and CMIP5 (bottom) simulated relationship between June-August Texas averaged rainfall departures (% of climatology) and surface temperature departures (°C). Left (right) panels show the relationship for 1981-2010 (2011). Each dot corresponds to the temperature/precipitation for a particular model realization. For AMIP, there are 360 (80) realizations for 1981-2010 (2011). For CMIP, there are 720 (220) realizations for 1981-2010 (2011). Inset values are for the correlation (R) and the slope (b) of the linear fit expressed as °C/%Pcpn departure. The blue wagon wheel denotes the observed JJA 2011 values.

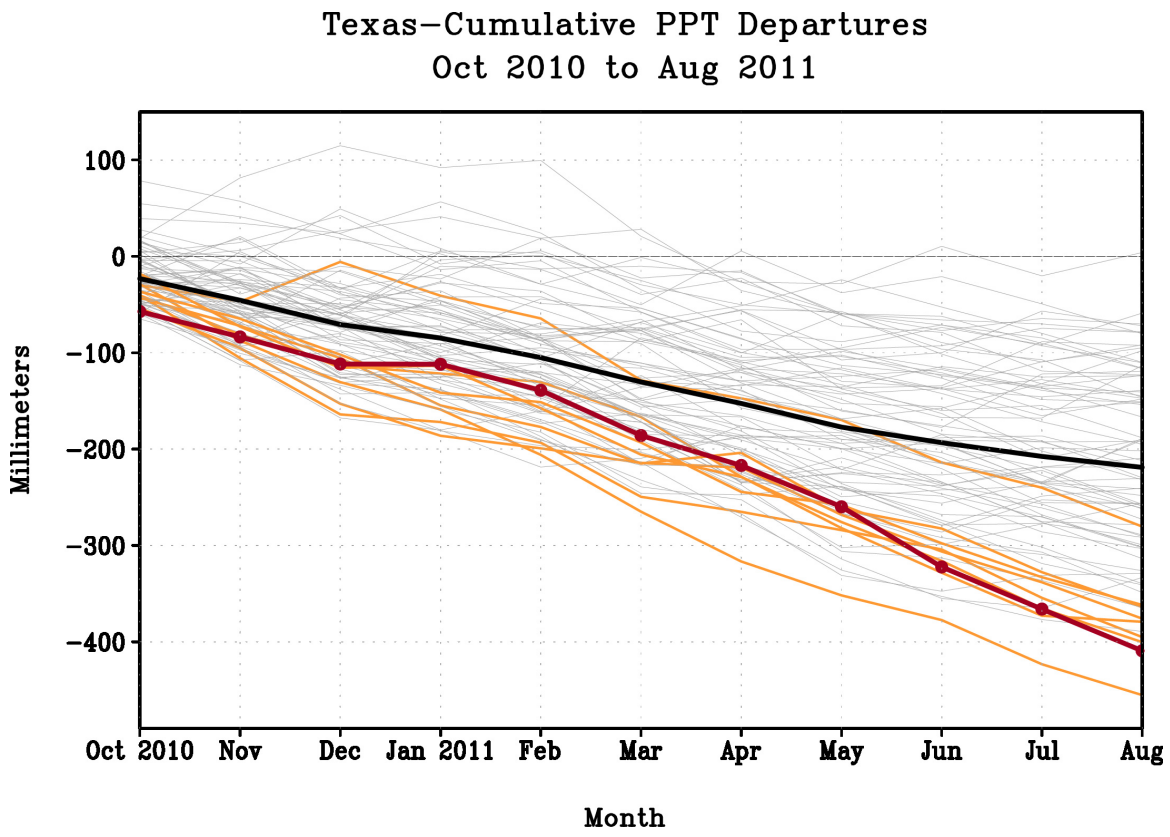

Figure 9. Observed (red curve) and AMIP ensemble mean (thick black curve) cumulative Texas precipitation departures (mm) from October 20110 through August 2011. Thin black curves are for each of the 80 members of the GFS AMIP simulations. Orange curves are the cumulative precipitation departures for the subset of 8 warmest Texas JJA 2011 GFS realization. Departures are computed relative to the respective data sets' 1981-2010 mean.

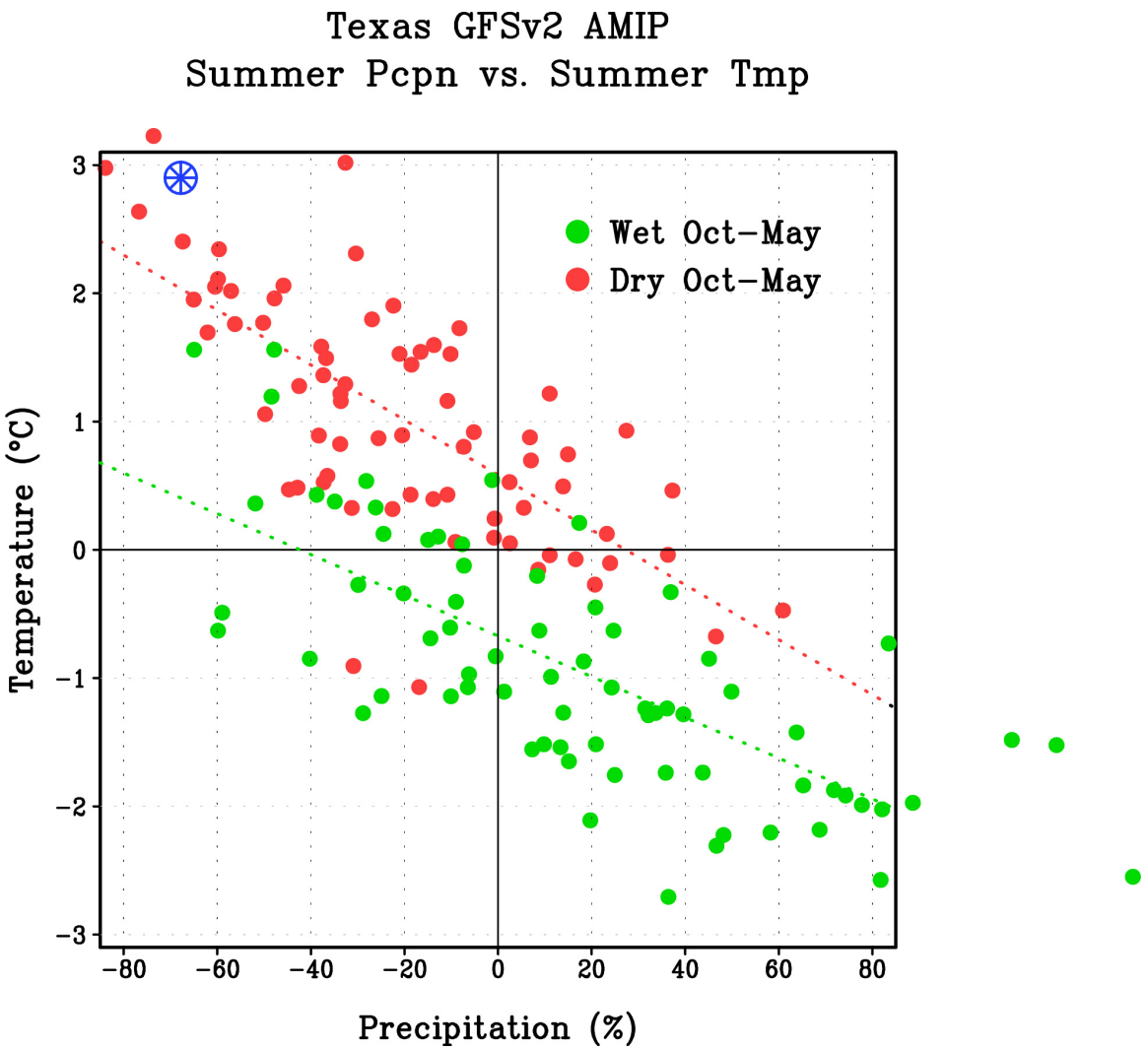

Figure 10. The simulated relationship between June-August Texas averaged rainfall departures (% of climatology) and surface temperature departures (°C) for wet (dry) Texas antecedent October-May conditions in green (red) dots. The data is based on the 12-member suite of 1950-2010 GFS AMIP simulations, and the plotted values are for the 10% wettest (driest) October-May realizations corresponding to 72 samples for each extreme.

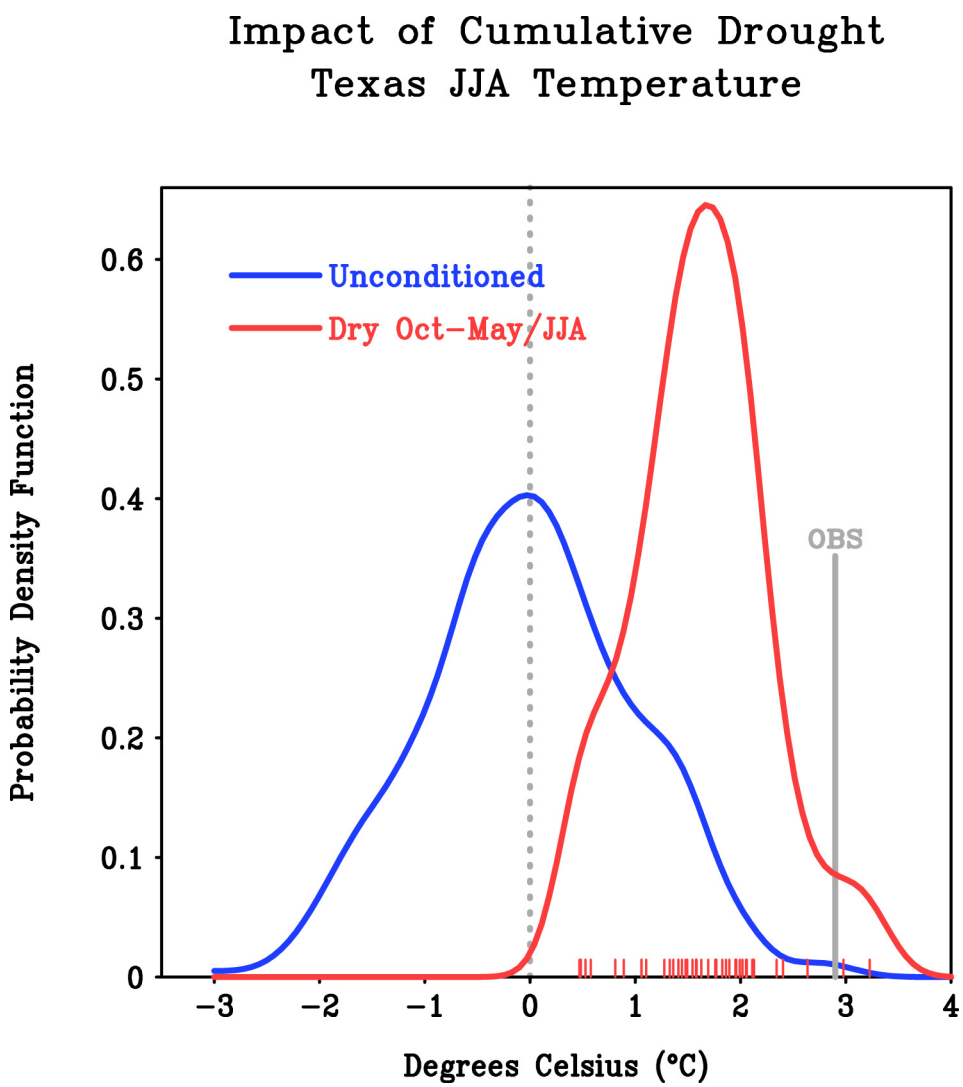

Figure 11. Probability distribution functions (PDFs) of GFS simulated June-August Texas surface temperature based on a joint condition of dry antecedent and dry summer conditions (red curve), and for unconditional model realizations (blue curve). Red PDF is comprised of the 41 realizations that were among both the driest 20% Oct-May and the driest 20% June-August conditions. Blue PDF is the unconditioned frequency distribution that is comprised of all 720 model realizations. Grey tic mark denotes the magnitude of the observed JJA 2011 Texas temperature departure.

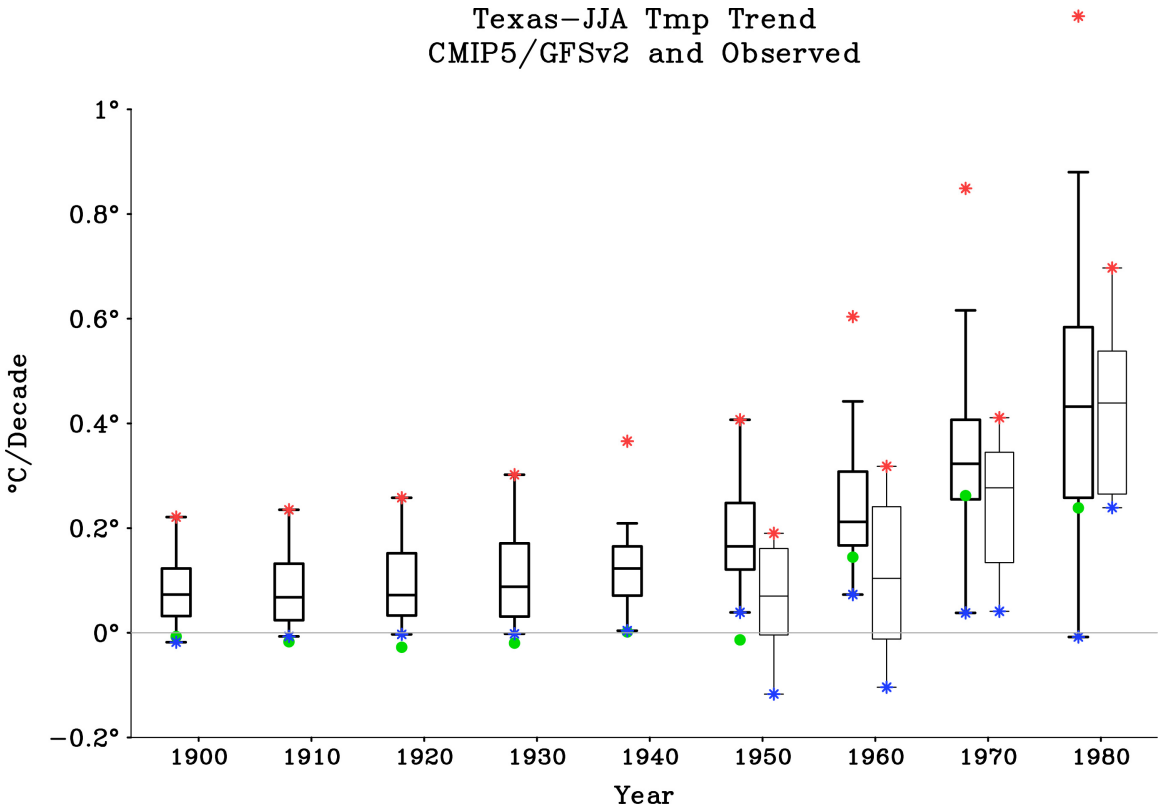

Figure 12. Observed (green dot) and simulated (box/whiskers) trends in June-August Texas surface temperature (°C/decade). Trends are computed for different beginning years from 1901 (left most box) to 1981 (right most boxes), staggered at 10-year increments, while the end year for all trend calculations is 2010 Thus, the longest trend period is for a 110-yr period (left side), and the shortest is for a 30-yr period (right side). Dark (light) box/whiskers display the CMIP5 (AMIP) simulation trends based on a 20-member (12-member) ensemble. The extreme values of the model simulated trends are shown by the red and blue asterikes.

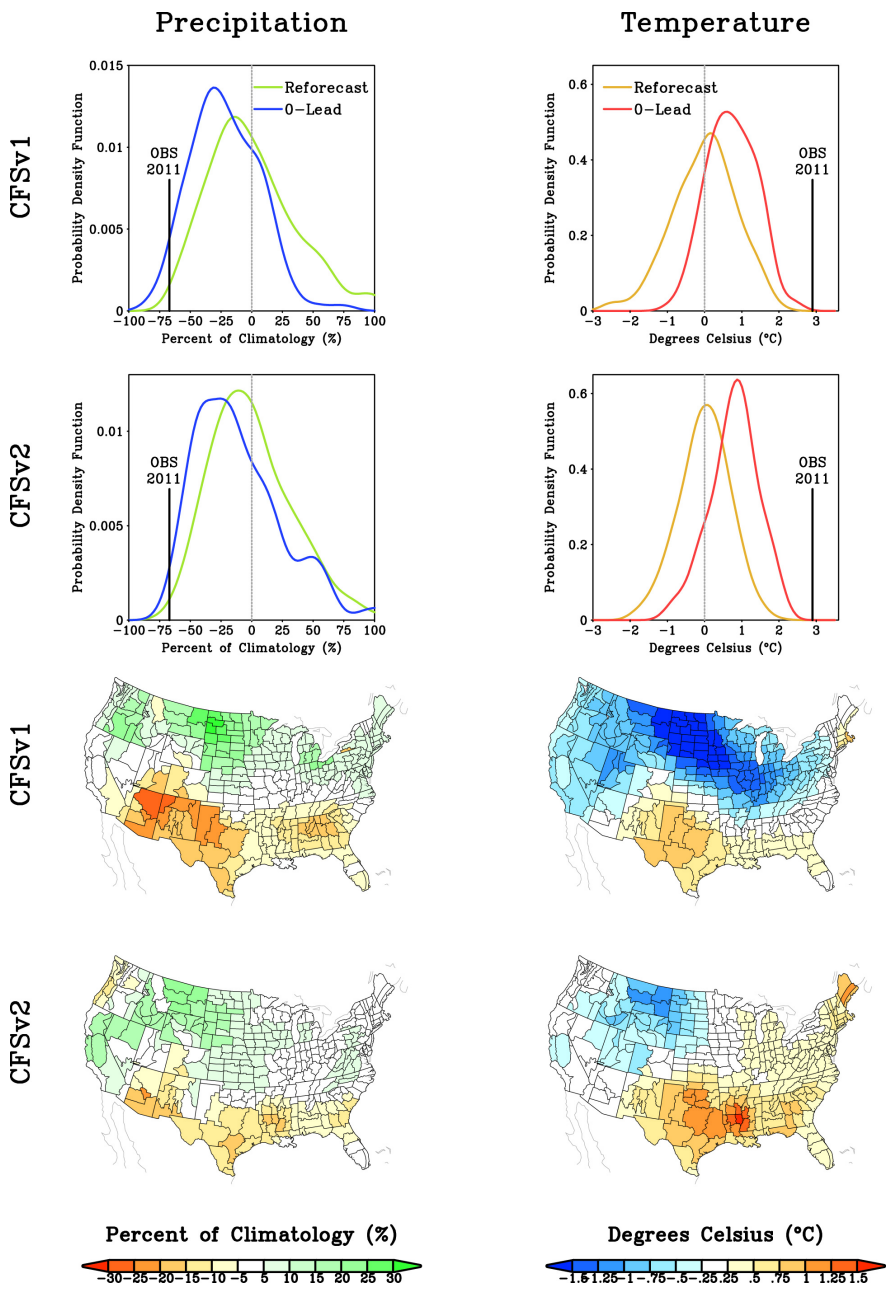

Figure 13. NOAA/NCEP operational dynamical predictions of June-August seasonally averaged precipitation anomalies (% of climatology, left) and surface temperature anomalies (°C, right). Probability distribution functions as in Fig. 7. Spatial anomaly maps as in Fig. 6, except based on the ensemble mean of the CFS forecasts. For CFSv1, 435 (124) individual hindcasts (forecasts) are used for 1981-2009 (2011). For CFSv2, 696 (124) individual hindcasts (forecasts) are used for 1982-2010 (2011). All hindcasts and forecasts are based on initializations from May analyses, and anomalies are calculated relative to the period of available hindcast climatologies for all May initializations.